A MULTISCALE MODELING APPROACH TO PREDICT THERMOPHYSICAL PROPERTIES OF HETEROGENEOUS MEDIA

MANUEL E. CRUZ[(1)] and CARLOS F. MATT[(2)]

[(1)]Department of Mechanical Engineering

Poli/COPPE/UFRJ

[(2)]Department of Equipment and Installations

CEPEL

Escola Sul-Americana PROPFIS

07/06/2005

Rio de Janeiro, RJ

AGRADECIMENTOS

- Alunos e Ex-alunos de Graduação e Pós-graduação
  - Alexandre Dallalana, Bruno Jesus da Costa e Alan Zaragoza Labes (IC)
  - Antonio Carlos Pinto Pereira e Leonardo Bernardo (IC)
  - Sílvia da Costa Hirata (IC, Proj. Final e M.Sc.)
  - Érico Fagundes Anicet Lisboa (M.Sc.)
  - Leandro Bastos Machado (Proj. Final e M.Sc.)
  - Rodrigo Penha Andrade Rocha (Proj. Final, M.Sc. e D.Sc. em andamento na COPPE)
  - **Carlos Frederico Trotta Matt** (M.Sc. e D.Sc.)
- Órgãos de Fomento
  - CNPq, FAPERJ, CAPES, FUJB/UFRJ

TÓPICOS DA APRESENTAÇÃO

- INTRODUÇÃO
  - Generalidades: Meios heterogêneos
  - Objetivos e Motivação
  - Problema de interesse
- BREVE REVISÃO DA LITERATURA
- O MÉTODO DE HOMOGENEIZAÇÃO
- CONDUÇÃO DE CALOR EM COMPÓSITOS
  - Descrição física
  - Formulação matemática (formas forte e fraca)
  - Aplicação da teoria da homogeneização
- ABORDAGEM MULTIESCALA
  - O problema da macroescala
  - O problema da mesoescala
  - O problema da microescala
- MÉTODOS NUMÉRICOS
  - Geração de malhas em 2-D e 3-D
  - Discretização por elementos finitos isoparamétricos
  - Métodos iterativos

INTRODUÇÃO

- Generalidades: Meios heterogêneos

Vamos nos convencer, simultaneamente, que o problema da **transferência** de calor em **meios heterogêneos**, em um contexto amplo, e o problema da **condução** de calor em **materiais compósitos**, em um contexto particular, são problemas extremamente idosos, relevantes, desafiadores, interessantes e atuais!

Desejamos entender, de fato, o **comportamento macroscópico** destes meios ou materiais, que depende de suas ‘propriedades efetivas.’

Phil. Mag.
34, 481-502
1892

LVI. *On the Influence of Obstacles arranged in Rectangular Order upon the Properties of a Medium.* *By* Lord RAYLEIGH, *Sec. R.S.**

THE remarkable formula, arrived at almost simultaneously by L. Lorenz † and H. A. Lorentz ‡, and expressing the relation between refractive index and density, is well known, but the demonstrations are rather difficult to follow, and the limits of application are far from obvious. Indeed, in some discussions the necessity for any limitation at all is ignored. I have thought that it might be worth while to consider the problem in the more definite form which it assumes when the obstacles are supposed to be arranged in rectangular or square order, and to show how the approximation may be pursued when the dimensions of the obstacles are no longer very small in comparison with the distances between them.

Taking, first, the case of two dimensions, let us investigate the conductivity for heat, or electricity, of an otherwise uniform medium interrupted by cylindrical obstacles which are arranged in rectangular order. The sides of the rectangle will be denoted by α, β, and the radius of the cylinders by a. The simplest cases would be obtained by supposing the material composing the cylinders to be either non-conducting or perfectly conducting; but it will be sufficient to suppose that it has a definite conductivity different from that of the remainder of the medium.

Fig. 1.

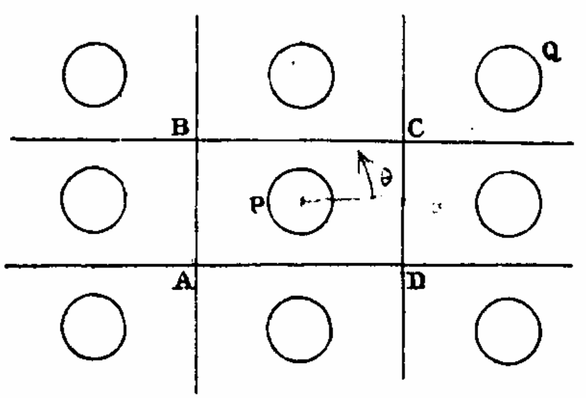

Proc. R. Soc. Lond. A **369**, 207–225 (1979)
Printed in Great Britain

Transport properties of regular arrays of cylinders

BY W. T. PERRINS, D. R. MCKENZIE AND R. C. MCPHEDRAN
School of Physics, University of Sydney, New South Wales 2006, *Australia*

(*Communicated by R. H. Brown, F.R.S. – Received* 20 *February* 1979 – *Revised* 22 *May* 1979)

We extend a method devised by Lord Rayleigh to enable the calculation of the transport properties of circular cylinders in square and hexagonal arrays. The theory is confirmed by measurements on arrays of perfectly conducting cylinders, and also is compared with asymptotic formulae due to Keller (1963) and O'Brien (1977). It is used to furnish plots of equipotential lines within the array. It is also applied to the calculation of the optical properties of films with columnar structure. Detailed studies for copper films show both the good solar selectivity possible with voided structures and the transition from a good reflector to a metal black consequent upon structural changes.

We give an analytic expression for the conductivity of this array in a similar forr to Rayleigh (1892) based on square truncation to order $N = 3$:

$$\epsilon = 1 - 2f \bigg/ \left[T + f - \frac{0.305827 f^4 T}{T^2 - (1.402958 f^8)} - \left\{ \frac{0.013362 f^8}{T} \right\} \right], \quad (14$$

where T is again defined by equation (13).

The term in curly brackets is the first correction term obtained from triangula truncation for order $N = 4$. It is to be noted that Rayleigh failed to include the terr in round brackets in his analytic expression based on the same order of summation

Journal of COMPOSITE MATERIALS, *Vol. 17—May 1983*

Thermal Conductivities of a Cracked Solid

ALAN HOENIG
Department of Mathematics
John Jay College of Criminal Justice
445 West 59th Street
New York, New York 10019

(Received January 18, 1983)

ABSTRACT

Formulas are presented which describe the effect of flat elliptical cracks on the effective thermal conductivity of an otherwise homogeneous body. The cracks are assumed randomly and isotropically distributed throughout the body, and may either be dry or composed of any material with a conductivity differing from that of the matrix. Effective conductivities depend solely upon a crack density parameter when the cracks are dry, and additionally upon a saturation parameter and the crack planform aspect ratio otherwise.

ANALYSIS

An analogy exists between σ, the electric conductivity, J and E, the curre and electric field vectors respectively, and between k, the thermal conducti ity, and q and grad T, the vector heat flow and temperature. Notice that i the governing equations describing the two phenomena, corresponding quai tities in the following lists play identical roles:

σ J E	k q grad T
$J = \sigma E$ div $J = 0$	$q = k(\text{grad } T)$ div $q = 0$

In the same way, one can show that this analogous behavior persists in tl specification of boundary conditions [3]. These observations imply that coı clusions about electric behavior apply to thermal problems when the substitu tions

$$J \rightarrow q$$
$$E \rightarrow \text{grad } T \quad (\,$$
$$\sigma \rightarrow k$$

are carried out. Hoenig [3] has presented a study of the effects of cracks o the electrical conductivities of bodies. These results can be applied to therma problems by means of the above substitutions. This analysis assumes tha heat transfer across dry cracks by radiation or convection will not take plac

The problem of determining k in (2) has been reduced by the above com ments to the problem of evaluating the expression (grad $T)/q^{\infty}$ for a singl crack and then averaging this expression over all orientations of the crack The process of evaluation must somehow take into account the influence o the other cracks of the body; this is done by invoking a *self-consisten hypothesis*, initially articulated by Budiansky [6] and Hill [7]. According tc their hypothesis, each crack in the matrix 'sees' itself as being embedded in aı uncracked body, characterized however by the as-yet-unknown effective con ductivity (that is, the macroscopic conductivity) of the cracked body. In thi manner, the difficult problem of evaluating the right-most factor of (2) in th context of a crack subject to the complex influence of neighboring cracks i replaced by the substantially simpler one of evaluating this factor by con sidering a single crack in a specially defined but homogeneous matrix. An im plicit assumption in this procedure is that the crack concentration is suffi ciently small so that the effect of crack intersections can be neglected.

HEAT AND MASS TRANSFER IN REFRIGERATION AND CRYOGENICS

Effective Thermal Conductivity of Frost

H. AURACHER
Institut für Technische Thermodynamik
und Thermische Verfahrenstechnik
Universität Stuttgart
Pfaffenwaldring 9
7000 Stuttgart 80, FRG

TRACT

a temperature gradient exists in a frost layer energy is nsferred from the warm to the cold side by molecular conducn, by water vapor diffusion, by radiation and occasionally by ural convection of the pore gas. A theoretical and experimen- study has been carried out on the influence of these differ- transport mechanisms on the total energy flux in frost. This al energy flux can be represented by an effective thermal con- tivity.

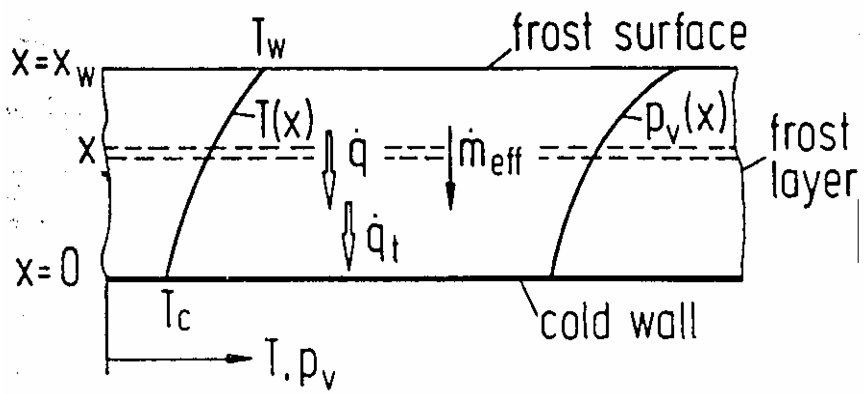

IGURE 1. Heat and mass fluxes in a frost layer

is useful to separate the different effects by defining indiv dual thermal conductivities

$$\lambda = - \frac{\dot{q}}{dT/dx} \quad ($$

and to finally add all relevant individual conductivities to c tain an effective thermal conductivity of frost.

These few examples show that based on the criteria mentioned a ove only under extreme system conditions an influence of natur convection may occur. Normally, in real situations, it can neglected. However, one has to take into account, that criter (15) and (18) are valid for closed porous spaces, which in ge eral is not the case with frost layers. Thus, a different beh vior of the convective flux is possible. This should be studi by special experiments in the future.

CONDUCTION

Molecular conduction in the ice matrix and in the pore space by far the most important effect on the total heat flux.

The thermal conductivity of frost is not only a function of de sity and temperature but also of its internal structure.

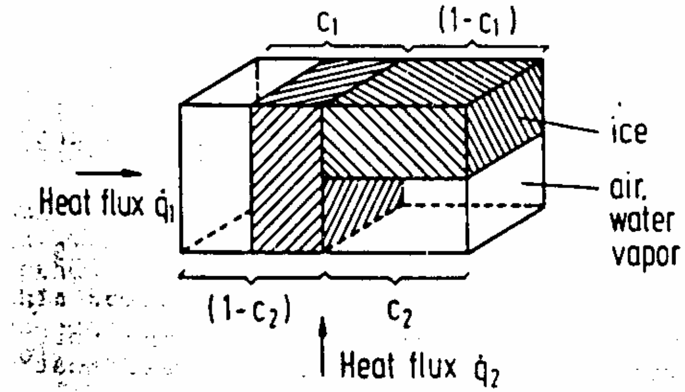

FIGURE 9. Frost structure model

EFFECTIVE THERMAL CONDUCTIVITY

From the foregoing considerations it follows that conduction an diffusion are the relevant effects on heat transfer in frost. Th effective thermal conductivity is thus given by

$$\lambda_{eff} = \lambda_{Cd} + \lambda_D \quad , \quad (27$$

with the thermal conductivity λ_D due to diffusion according t eq. (10) (see Fig. 2) and the conduction thermal conductivit λ_{Cd} from eq. (21) considering eqs. (14), (19), (20), (23), (24 and (25).

JOURNAL OF MATERIALS SCIENCE 22 (1987) 701–709

Heat conduction characteristics of a carbon-fibre-reinforced lithia–alumino–silicate glass–ceramic

D. P. H. HASSELMAN*, L. F. JOHNSON*, R. SYED*, MARK P. TAYLOR‡, K. CHYUNG‡
*Department of Materials Engineering, Virginia Polytechnic Institute and State University, Blacksburg, Virginia 24061, USA
‡Corning Glass Works, Corning, New York 14830, USA

A study was conducted of the thermal diffusivity, specific heat and thermal conductivity of a uniaxially carbon-fibre-reinforced lithia–alumino–silicate glass–ceramic. The thermal diffusivity and conductivity parallel to the fibre direction was found to be independent of thermal history and more than an order of magnitude higher than in the transverse directions. During the first thermal cycle, the thermal diffusivity transverse to the fibre direction was found to exhibit a decrease attributed to crack formation under the influence of internal stresses. The transverse thermal diffusivity on thermal cycling to 1000° C exhibited lower values during heating than during subsequent cooling. This hysteresis was attributed to a thermal history-dependent barrier to heat flow at the matrix–fibre interface. The thermal conductivity of the fibres along their length inferred from composite theory was found to be much lower than the corresponding value for pyrolytic graphite, attributed to less than complete graphitization and associated high density of lattice defects which act as phonon scatterers.

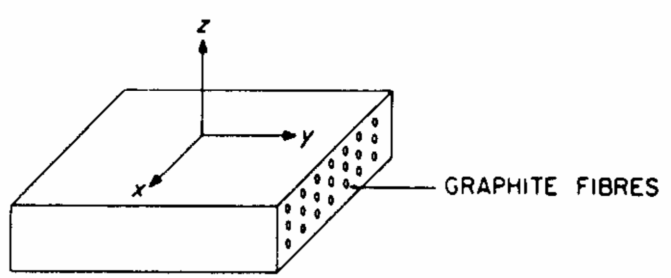

Figure 1 Orientation of carbon-fibre reinforced lithium–alumina–silicate glass-ceramic.

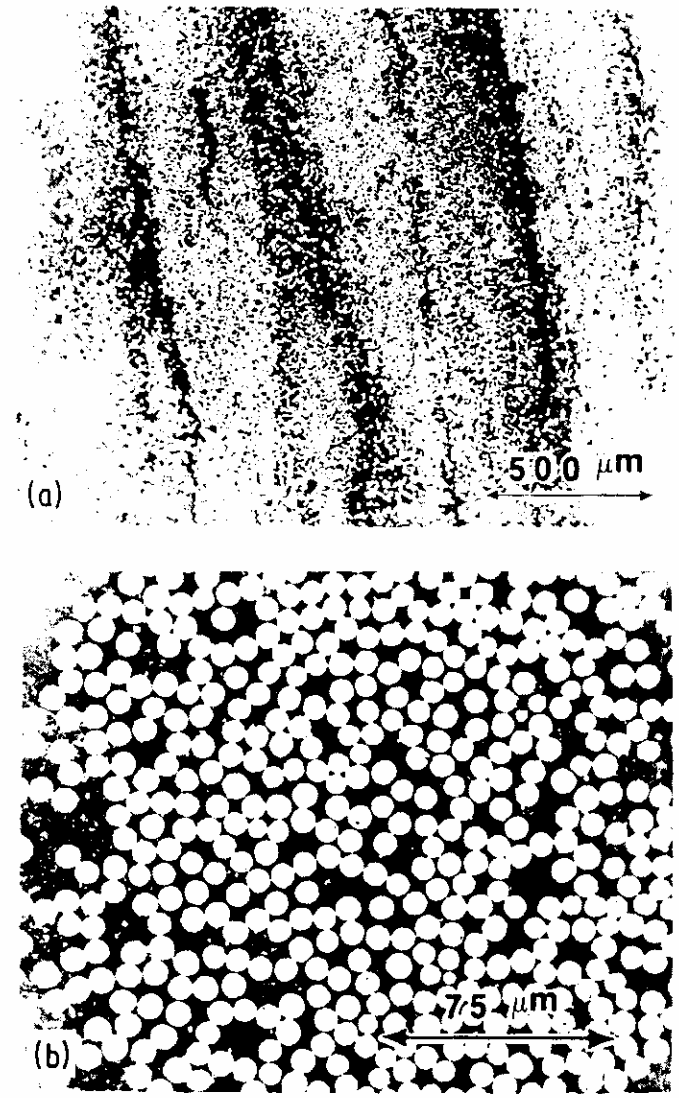

Figure 2 Photomicrographs of carbon fibre-reinforced lithia–alumino–silicate glass-ceramic at two different magnificati

Journal of COMPOSITE MATERIALS, *Vol. 26, No. 5/1992*

Thermal Diffusivities of Composites with Various Types of Filler

HIROSHI HATTA*
Materials and Electronic Devices Laboratory
Mitsubishi Electric Corporation
1-1-57 Miyashimo, Sagamihara
Kanagawa 229, Japan

MINORU TAYA**
Department of Mechanical Engineering
University of Washington
Seattle, WA 98195

F. A. KULACKI AND J. F. HARDER
College of Engineering
Colorado State University
Fort Collins, CO 80523

(Received June 1, 1990)
(Revised April 23, 1991)

ABSTRACT: In-plane and out-of-plane thermal diffusivities (conductivities) of Kerimid resin composites reinforced with various types of filler were studied both experimentally and theoretically. The types of filler used are SiO_2 particle, Al_2O_3 short fiber, Boron Nitride (BN) flake, and Si_3N_4 whisker. The prediction based on our previous model (Eshelby's equivalent inclusion method) agreed reasonably well with the experiment, except for BN flake composite. It was found that the orientation of filler has a strong effect on the overall thermal conductivity of a composite.

Among these thermal properties, thermal diffusivity (or conductivity) has been studied analytically by a number of researchers, for example, References [6–10]. These analytical models are, however, aimed at simple geometries of filler microstructure, such as unidirectionally oriented continuous fiber and spherical particle composites. Thus, in this paper, the thermal diffusivity of composites with more complicated types of filler geometry is studied both experimentally and analytically.

THEORETICAL ANALYSIS

Measured values of thermal diffusivity are compared with predicted val[ues] based on our model for thermal conductivity, k_c, of a misoriented short fi[ber] composite [3,4].

The orientation distribution of the filler can be easily estimated by consider[ing] that all the composite samples were formed by compression molding. That is [to] say, short fiber and whisker composites can be considered to be nearly tw[o-] dimensional (2D random) and flake composites, unidirectional. The thermal co[n]ductivity of a composite reinforced with fillers of given orientation type can [be] predicted by our model based on Eshelby's equivalent inclusion model [3,4]. [In] this model, actual fillers with thermal conductivity k_f in a composite are replac[ed] by equivalent inclusions which possess the same thermal conductivity as the s[ur]rounding matrix, k_m, and eigen-temperature gradient. Thus, the model is simi[lar] to that developed originally for elasticity problems [17,18]. The present study [in]cludes:

1. Spherical particle reinforced composite (SiO_2 particle/Kerimid)
2. In-plane random short fiber reinforced composite (BN flake/Kerimid)
3. 2D random short fiber reinforced composite (Al_2O_3 short fiber/Kerim[id], Si_3N_4 whisker/Kerimid)
4. Nearly three-dimensional (3D random) short fiber reinforced compos[ite] (Si_3N_4 whisker/Kerimid)

EXPERIMENTAL APPARATUS AND PROCEDURE

Sample Selection and Preparation

Four kinds of fillers and heat resistant polymers (Table 1) which exhibit rel[a]tively high thermal conductivity, were chosen for the reinforcement and matri[x], respectively.

In the selection process, special attention was place[d] upon covering a wide range of filler geometry, i.e., from flake to short fiber. Th[e] raw materials were processed into composite materials by two kinds of compre[s]sion molding methods, the premix method and the paper making method,

It should be noted in the figure that, except fo[r] BN/Kerimide composite [Figure 8(c)], the predicted values of λ_z and λ_{xy} agre[e] reasonably well with the experimental values when the volume fraction of th[e] filler V_f is small, but overestimate the experimental values as V_f becomes large

JOURNAL OF THERMOPHYSICS AND HEAT TRANSFER
Vol. 14, No. 2, April-June 2000

Conduction and Radiation Heat Transfer in High-Porosity Fiber Thermal Insulation

Siu-Chun Lee and George R. Cunnington
Applied Sciences Laboratory, Inc., Hacienda Heights, California 91745

Radiation is the primary mode of heat transfer in high-porosity fiber thermal insulations even at temperatures above a few hundred Kelvin. Consequently, many studies have reported on the modeling of radiation heat transfer through high-porosity fibrous media.

Heat transfer by combined radiation and conduction in fibrous media has been addressed by many investigators using a simple additive model in terms of the thermal conductivities for radiation and conduction; the latter includes conduction through the solid lattice of the fiber medium and any gas present in the insulation.

The present theoretical radiation model includes formulations for radiative properties and thermal conductivity of fibrous media.

Fig. 3 SEM of bonded fibers; magnification = 1200X.

Conduction Heat Transfer

Although the dominant mode of heat transfer through high-porosity fiber thermal insulations is generally radiation, the contributions of conduction through the solid phase, i.e., fibers, and any gas present in the void space between the fibers must be accounted for when comparing theoretical predictions with measured heat-transfer data.

In the limit of large optical thickness, Eq. (35) reduces to

$$k_e = k_r + k_c \tag{39}$$

indicating that heat transfer by radiation and conduction are additive for optically thick media.

JOURNAL OF THERMOPHYSICS AND HEAT TRANSFER
Vol. 14, No. 2, April-June 2000

Determination of Spectral Radiative Properties of Open Cell Foam: Model Validation

D. Baillis,* M. Raynaud,† and J. F. Sacadura‡
Centre National de la Recherche Scientifique, 69621 Villeurbanne Cedex, France

Spectral radiative properties (absorption coefficient, scattering coefficient, and phase function) of open cell carbon foam are determined experimentally. The identification method uses spectral transmittance and reflectance measurements and a prediction model based on a combination of geometric optics laws and of diffraction theory. In the wavelength region of 0.1–2.1 μm, directional–hemispherical transmittance and reflectance measurements are used, whereas directional–directional transmittance and reflectance measurements are used in the wavelength region of 2–15 μm. Thus, radiative properties are determined in the wavelength region from visible to infrared. The two approaches corresponding to the two different types of measurement (directional–directional and directional–hemispherical) are compared for the determination of radiative properties. Moreover, experiments performed on a guarded hot-plate-type device are used to confirm that the proposed model is appropriate to predict the radiative heat transfer in such media.

Open cell carbon foam can be used as efficient thermal insulation for high-temperature applications. Insulating foam consists of a highly porous solid material. Open cell foam insulations are semitransparent media (absorbing, emitting, and scattering radiation).

To model heat transfer in such media, it is necessary to determine radiative and conductive properties.

The total conductivity includes the three independent mechanisms: conduction through the gas, conduction through the solid material forming the cell, and thermal radiation[13–15]:

$$k_t = k_{\text{gas}} + k_{\text{solid}} + k_r \qquad (7)$$

37th Thermophysics Conference
28 June – 1 July 2004, Portland, Oregon

AIAA 2004-2571

Effective Thermal Conductivity of Saturated

Sintered Nickel Loop Heat Pipe Wicks

by

M. Bonnefoy and J. M. Ochterbeck*
Mechanical Engineering Department
Clemson University
Clemson, SC 29634-0921

B. L. Drolen
Boeing Satellite Systems
Los Angeles, CA

M. N. Nikitkin
Swales Aerospace
Beltsville, MD

Abstract

In this investigation, the effective thermal conductivity of sintered metal wicks was studied both experimentally and analytically. The experimental study consisted of measuring the effective conductivity of eleven samples in vacuum and with three different saturating fluids (air, water and methanol). The analytical study aimed to find a model to better predict the effective conductivity. The wicks tested were typical of loop heat pipes for spacecraft thermal control systems. The data obtained using the different fluids allows the effective thermal conductivity to be predicted as a function of other saturating fluids. The measured values for effective thermal conductivity were compared with other typically measured parameters for loop heat pipe wicks, including the porosity, permeability, pore radius, and compression load.

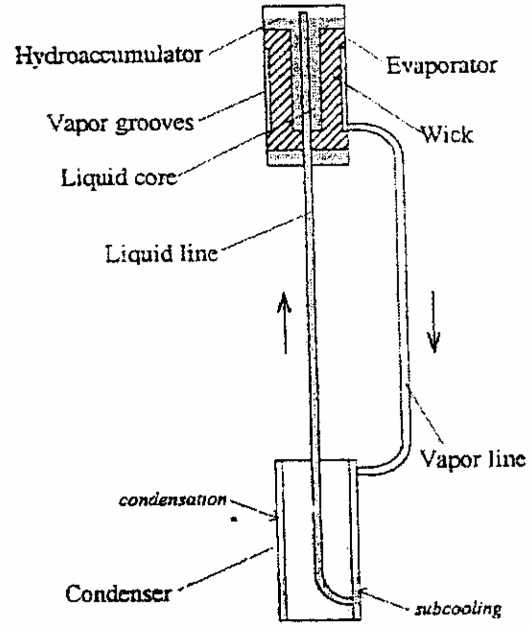

Figure 1: Basic Loop Heat Pipe [2]

Models of Effective Thermal Conductivity

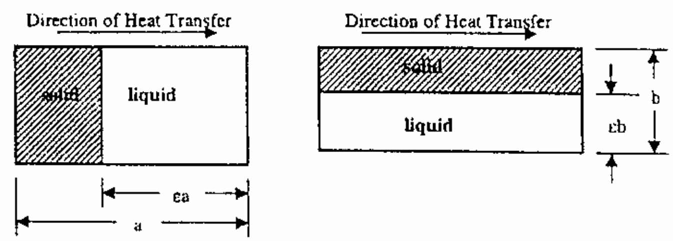

a) b)

Figure 2 a) liquid and solid in series, b) liquid and solid in parallel [4]

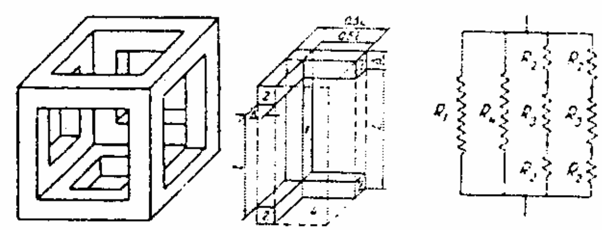

a) b) c)

Figure 3 : a) unit cell, b) a quarter of the unit cell, c) heat resistance schematic [7]

Effective Thermal Conductivity of Liquid Satura
Sintered Fiber Metal Wicks

The e
on the measurement of the thermal resistance of
wick was less than 9.1% as shown by calculatio

Overall Results

Comparison was made between the mentioned b
models for the effective conductivity and
experimental results. Most models were unabl
accurately predict the effective conductivity, both ir
and saturated states.

One item to note is that
correlations typically only use the sample porosit
vary the effective conductivity. This results in signific
lost information regarding the sample structure.

Conclusions and Recommendations

In future work, additional measurements of the effe
conductivity with variations in the metal material ar
alternate to water would be beneficial. As
development of a correlation, information regardin
structure of the samples is seen as vital.
information consists of the particle size distributior
general particle geometry (it is assumed the par
are not really spherical based on the current resu
the measurements).

Materials Transactions, Vol. 45, No. 2 (2004) pp. 542 to 549

icrostructural Modeling and Thermal Property mulation of Unidirectional Composite

iko Kikuchi[1], Yan-Sheng Kang[1], Akira Kawasaki[1], Shinya Nishida[2] and Akira Ichida[2]

partment of Materials Processing, Graduate School of Engineering, Tohoku University, Sendai 980-8579, Japan
.M.T. Corp., Toyama 931-8543, Japan

The electrical, thermal and mechanical properties of functionally graded materials vary with microstructure and composition. sequently it is very important to know quantitatively the properties of composites for the design of functionally graded materials. However, methods of quantitative and theoretical evaluation for material properties on wide compositional range have been established. In this arch, a method that estimates the material properties of composites directly from their microstructure assisted with finite element analysis investigated. As an example of the estimation of material properties, the thermal conductivity of Mo fiber-Cu matrix composites has been uated. Calculated results of thermal conductivity are well in agreement with the experimental data measured by using a laser flash apparatus the smallest deviation is 1.9%. The finite element analysis using a metallographic model is a very accurate method for estimation of posite properties.

Digital Image Based (DIB) metric modeling technique[10,12] was used to reflect the ıal morphology of composite microstructure such as usion shape, volume fractions, etc. on Finite Element) model. The DIB technique for 2-dimensional models be divided into three parts.

s DIB technique has a great advantage of excluding any shing manipulation such as defining coordinates and ment connectivities because all the elements have the ıe size.

Fabrication and evaluation of Mo fiber-Cu matrix composite

Io fiber-Cu matrix composite specimens were prepared n Mo fibers with a diameter of 120 μm and Cu plates.

(a)

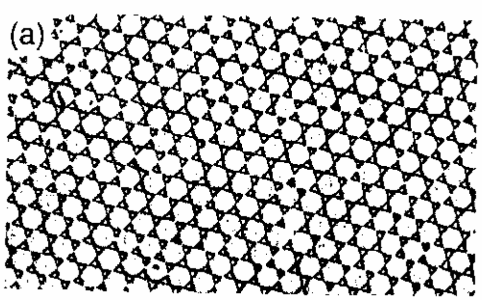

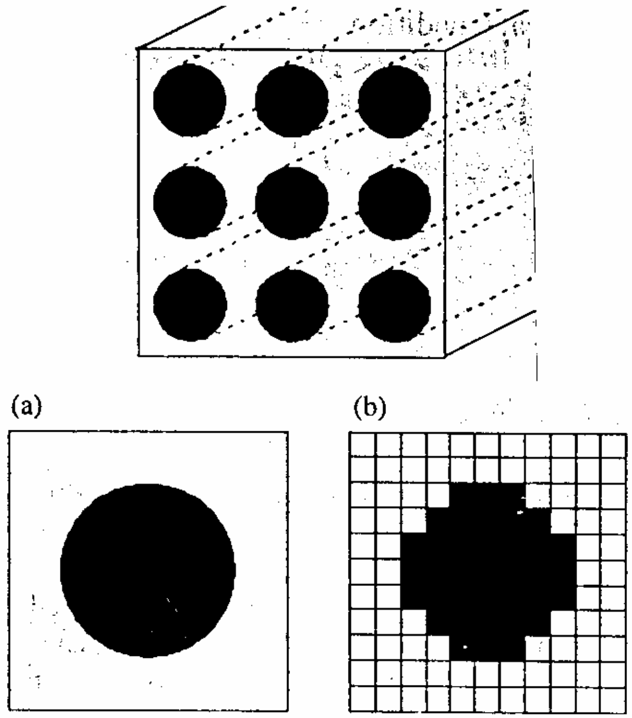

Fig. 3 The schematic illustration of the unidirectional model for circular cylinders packed in square arrays. (a) a unit cell. (b) the schematic illustration of FE model based on unit cell (a).

Thermal Conductivities of the Ideal Model Unidirectional Composite

Modeling of ideal microstructure

The model of unidirectional circular cylinders pack square arrays is shown as an ideal unidirectional compos Fig. 3. From this ideal model, it is assumed that (a composites are macroscopically homogeneous, (b) lo both the matrix and the fiber are homogeneous and iso (c) the thermal contact resistance between the fibe matrix is negligible, (d) the problem is two-dimensiona (e) the fibers are arranged in a square periodic array, *i.e* are uniformly distributed in the matrix. The model sho Fig. 3(a) is a unit cell which represents one-cycle periodic structure, so the transverse thermal conducti unidirectional composite of circular cylinders was esti by using this unit cell. The unit cell was divided into 4 fixed size square elements as shown in Fig. 3(b), so th FE model obtained from the unit cell became equiva that obtained from the microstructure of composites.

Comparison

The fibrous and transverse thermal conductivities c specimens were plotted respectively in Fig. 11, wher volume fraction of molybdenum was determined to be from the density measured by Archimedes's method experimental thermal conductivity along the fiber dire was compared with the pararell model in Fig. 11(a), whi the transverse direction it was compared with the Per model in Fig. 11(b). The pararell model is a linear ru mixtures, while the Perrins's model is a predictive mod the transverse circular cylinders packed in hexagonal a Each experimental result is well in agreement wit predicted one, so there is no thermal barrier at the inter which is also obvious from the SEM micrographs.

INTRODUÇÃO (cont.)

- Objetivos

  Desenvolvimento e aplicação de uma abordagem multiescala analítico-numérica para cálculo da condutividade térmica efetiva de materiais compósitos com microestruturas 2-D ou 3-D e com ou sem a presença de uma resistência térmica interfacial

- Motivação

  Aplicabilidade prática de materiais compósitos em várias indústrias e produtos de alta tecnologia

  - Facilidade de fabricação
  - Baixo custo e baixo peso
  - Propriedades mecânicas, térmicas e elétricas desejáveis (rigidez, resistência à corrosão e ao desgaste, condutividade térmica, coeficiente de expansão térmica, constante dielétrica)

INTRODUÇÃO (cont.)

- Problema de interesse

  Condução de calor em regime permanente em materiais compósitos

- Definição de materiais compósitos
  - Meios heterogêneos fabricados com duas ou mais fases com propriedades macroscópicas distintas
  - Fase contínua: matriz (constituída por materiais metálicos, orgânicos ou cerâmicos)
  - Fase dispersa: partículas e/ou fibras (carbeto de silício, nitreto de alumínio, óxido de alumínio, grafite), vazios

- ‘Classificação’ dos materiais compósitos
  - Particulados (partículas [aprox.] esféricas, elipsoidais etc.)
  - Fibrosos (e.g., fibras com geometria axissimétrica)
  - Híbridos (mistura de partículas e fibras)

Carbon Fiber Composites

Deborah D. L. Chung

Butterworth–Heinemann © 1994

Boston London Oxford Singapore Sydney Toronto Wellington

Composite materials refer to materials containing more than one phase
ch that the different phases are artificially blended together.

A composite material typically consists of one or more fillers in a certain
atrix. A carbon fiber composite refers to a composite in which at least one of
e fillers is carbon fibers, either short or continuous, unidirectional or
ultidirectional, woven or nonwoven. The matrix is usually a polymer, a
etal, a carbon, a ceramic, or a combination of different materials.

Polymer-matrix composites are much easier to fabricate than metal-
atrix, carbon-matrix, and ceramic-matrix composites, whether the polymer is
thermoset or a thermoplast.

Carbon fiber metal-matrix composites are gaining importance because the
arbon fibers serve to reduce the coefficient of thermal expansion (Figure 7.1
[1]), increase the strength and modulus, and decrease the density. If a
elatively graphitic kind of carbon fiber is used, the thermal conductivity can be
nhanced also (Figure 7.2 [2]).

Carbon fibers used for metal-matrix composites are mostly in the form of
ontinuous fibers, but short fibers are also used.

Carbon is the matrix that is most compatible to carbon fibers.

In addition to having attractive mechanical prop-
ties, carbon–carbon composites are more thermally conductive than carbon
er polymer-matrix composites.

Carbon–carbon composites with high thermal conductivity are important
r first wall components for nuclear fusion reactors, hypersonic aircraft,
issiles and spacecraft, thermal radiator panels, and electronic heat sinks.

Carbon fibers are electrically and thermally conductive, in contrast to
nonconducting nature of polymer and ceramic matrices. Therefore, ca
fibers can serve not only as a reinforcement, but also as an additive
enhancing the electrical or thermal conductivity. Furthermore, carbon f
have nearly zero coefficient of thermal expansion, so they can also serve a
additive for lowering the thermal expansion. The combination of high the
conductivity and low thermal expansion makes carbon fiber composites u
for heat sinks in electronics and for space structures that require dimens
stability. As the thermal conductivity of carbon fibers increases with the de
of graphitization, applications requiring a high thermal conductivity shoul
the graphitic fibers, such as the high-modulus pitch-based fibers and the v
grown carbon fibers. Carbon fibers are more cathodic than practically
metal, so in a metal matrix, a galvanic couple is formed with the metal a
anode. This causes corrosion of the metal. The corrosion product tends t
unstable in moisture and causes pitting, which aggravates corrosion
alleviate this problem, carbon fiber metal-matrix composites are often coa

Thermal Conductivity

The the
conductivities of P-100, P-120, and K1100X fibers are all higher than tha
copper, while the thermal expansion coefficients and densities are much lo
than those of copper. Thus, the specific thermal conductivity is exceptio
high for these carbon fibers.

In contrast, v
grown carbon fibers have a thermal conductivity of 1 900 W/m/K at 25°C
Hence, carbon–carbon composites using vapor grown carbon fibers may h
thermal conductivity exceeding 1 000 W/m/K [77]. The low density of ca
makes the specific thermal conductivity of carbon–carbon composites outs
ingly high compared to other materials. The use of porous carbon–ca
composites with even lower densities [78] may further increase the sp
thermal conductivity.

Interface

Therefore, an optimum degree of fiber–matrix bonding is needed
brittle-matrix composites, whereas a high degree of fiber–matrix bondin
preferred for ductile-matrix composites.

The mechanisms of fiber–matrix bonding include chemical bonding,
der Waals bonding, and mechanical interlocking.

INTRODUÇÃO (cont.)

- Condutividade térmica efetiva (tensor de segunda ordem)

  "Razão" entre a média volumétrica do fluxo de calor e a média volumétrica do gradiente de temperatura em um elemento de volume representativo (Milton, 2002)

$$<\mathbf{q}> = \mathbf{K}_{\text{eff}} <\nabla T>$$

$$<\mathbf{q}> \equiv \frac{1}{V}\int_V q(\mathbf{x})\,dV = \frac{1}{V}\left(\int_{V_m}\mathbf{q}_m(\mathbf{x})\,dV + \int_{V_d}\mathbf{q}_d(\mathbf{x})\,dV\right)$$

$$<\nabla T> \equiv \frac{1}{V}\int_V \nabla T(\mathbf{x})\,dV = \frac{1}{V}\left(\int_{V_m}\nabla T_m(\mathbf{x})\,dV + \int_{V_d}\nabla T_d(\mathbf{x})\,dV\right)$$

(*m* – matrix; *d* – fase dispersa)

INTRODUÇÃO (cont.)

- Resistência térmica interfacial
  - Origem: processo de fabricação
  - Causas: aderência mecância e/ou química ruim; presença de impurezas e rugosidades; diferença entre os coeficientes de expansão térmica das fases; ruptura
  - Efeito: salto do campo de temperatura na interface entre as fases (barreira à condução de calor)
  - Definição/modelo: razão entre o salto de temperatura e o fluxo de calor na interface

$$R_I \equiv \frac{T_m|_{\text{interface}} - T_d|_{\text{interface}}}{q|_{\text{interface}}} \quad [\mathrm{m}^2 \cdot \mathrm{K/W}] \qquad h_s \equiv \frac{1}{R_I} \quad [\mathrm{W/m}^2 \cdot \mathrm{K}]$$

INTRODUÇÃO (cont.)

- Microestrutura

  Arranjo geométrico das fases do compósito; caracterizada pelo volume e pelas distribuições de posição, tamanho, orientação e forma da(s) fase(s) dispersa(s) no interior da matriz; a microestrutura pode ou não ser estatisticamente homogênea (⇨ fração volumétrica da fase dispersa independe da posição)

- Classificação para modelagem
  - ➢ Quanto à função de distribuição espacial das fases
    - ✓ Ordenada (função de distribuição ‘trivial’)
    - ✓ Randômica (função de distribuição ‘não trivial’)
  - ➢ Quanto à periodicidade
    - ✓ Periódica (elemento de volume representativo se repete ao longo das direções espaciais)
    - ✓ Não periódica

INTRODUÇÃO (cont.)

- Ilustrações de microestruturas 2–D (fase dispersa constituída por cilindros de comprimento 'infinito')

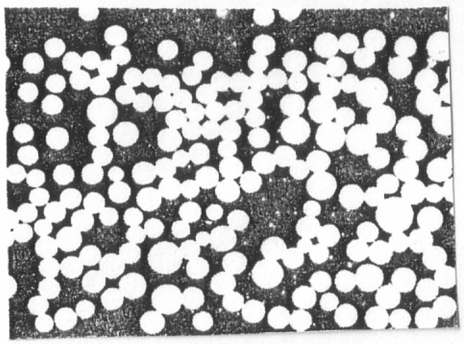

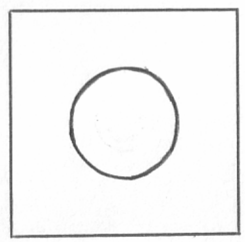

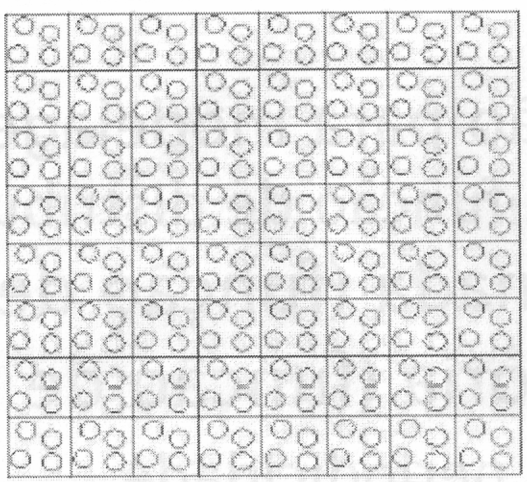

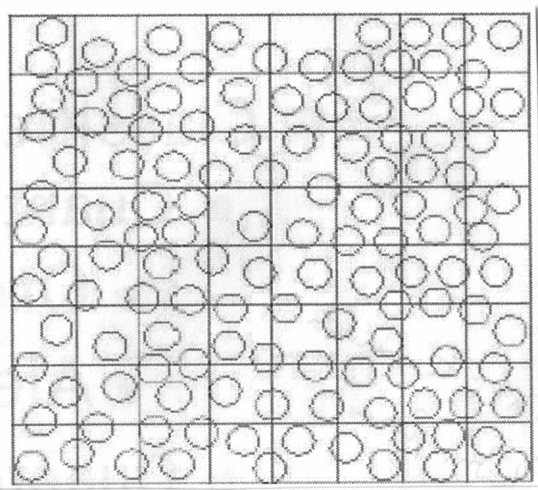

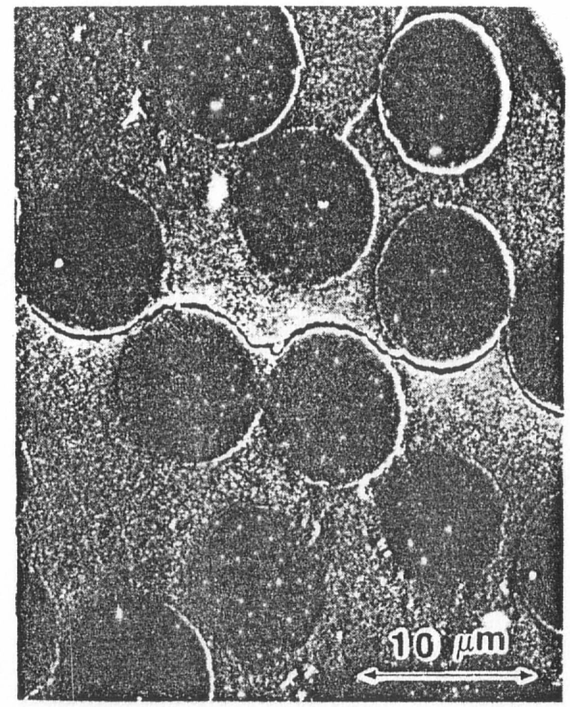

Figure 9 Crack formation in uniaxial carbon fibre reinforced lithi alumino–silicate glass-ceramic annealed for 4 h at 1000° C.

INTRODUÇÃO (cont.)

- Ilustrações de microestruturas 3-D
  (fase dispersa constituída por esferas)

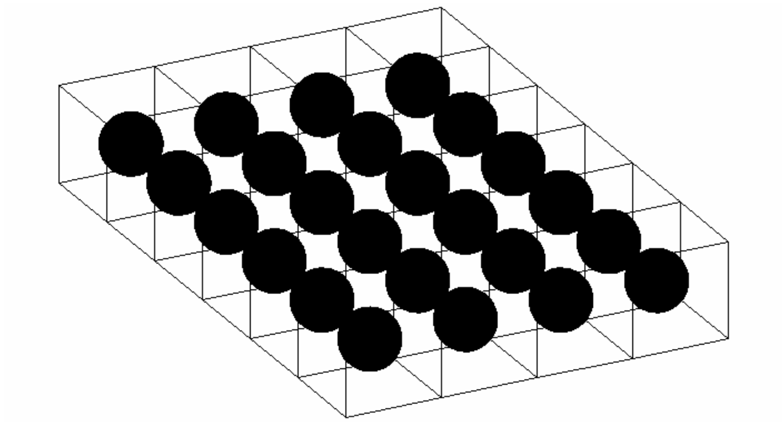

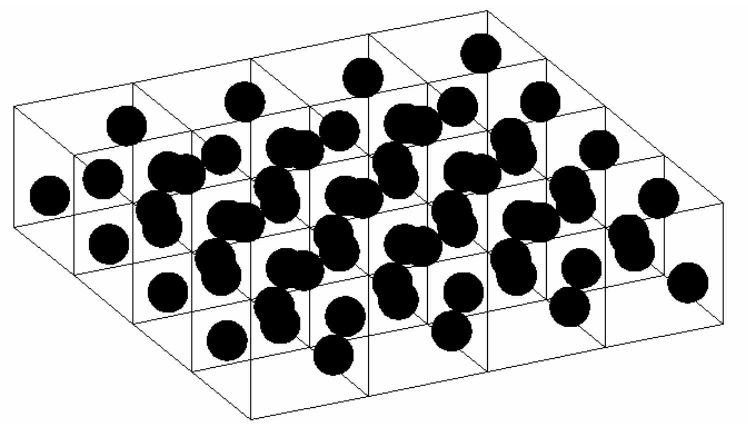

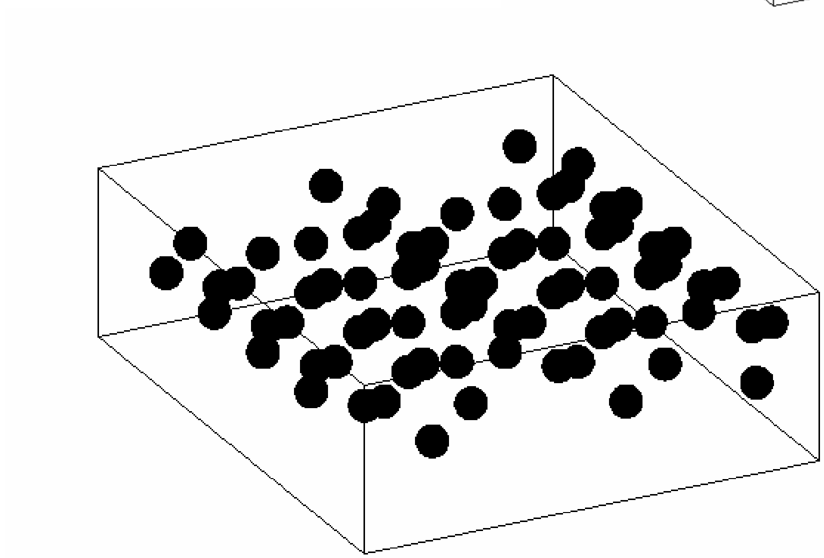

OURNAL OF MATERIALS SCIENCE 11 (1976) 2105–2141.

Review

The physical properties of composite materials

. K. HALE
ivision of Chemical Standards, National Physical Laboratory, Teddington,
iddlesex, UK

The coefficient of thermal conductivity is efined by Fourier's law which for an isotropic edium may be written in the form

$$J = -\lambda \operatorname{grad} T \tag{3}$$

here λ, the thermal conductivity, is the proortionality constant between the heat flux ector $\mathbf{J}$ and the temperature gradient. Other ansport coefficients are defined in a similar ay as proportionality constants between fluxes d gradients. Examples are the electrical conducvity (Ohm's law) and diffusion coefficients Fick's law).

With a composite material, the relations derived r all these properties will be formally identical d the expressions obtained for the dielectic nstant, for example, will be equally applicable the thermal conductivity or magnetic ermeability.

A large number of empirical or semimpirical expressions for the thermal conductivity heterogeneous systems have also been amined. As with the dielectric constant it will, owever, only be possible to obtain a satisfactory scription of the thermal conductivity behaviour taking the geometry of the composite into nsideration and making proper use of the geoetrical information that is available.

Problems of heat transfer are of considerable technological importance in situations where heat transfer has to be encouraged, as in heat exchangers, or reduced by the use of insulation. Most insulating materials are, indeed, essentially mixtures of a solid material and air and owe their insulating properties to the low thermal conductivity of air. The insulating material can have a fibrous or granular structure (e.g. glass wool or diatomaceous earth) in which case the air is the continuous phase or it can be cellular (e.g. a polyurethane foam). In the latter case, if the pores are open there will be two continuous phases; if they are closed there will be one continuous solid phase.

For a foamed or porous material, the thermal conductivity λ is often expressed as

$$\lambda = \lambda_s + \lambda_g + \lambda_r + \lambda_c \tag{40}$$

where λ_s, λ_g, λ_r and λ_c are contributions due to conduction through the solid, conduction through the gas, radiation and convection within the pores. This description is, however, misleading since it implies that the four processes are taking place independently and in parallel. At normal temperatures, however, radiation effects will be small and, if the cell diameter is less than 3 to 4 mm, convection effects will be negligible [43].

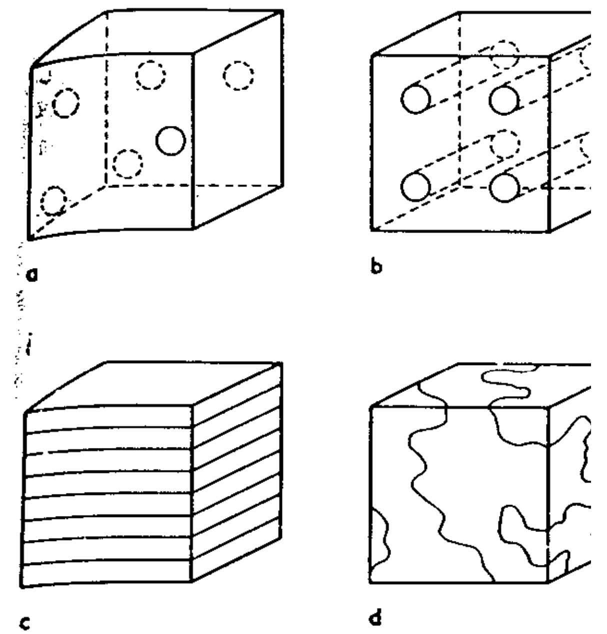

Figure 1 Composite geometries: (a) random dispersi spheres in a continuous matrix, (b) regular arra aligned filaments, (c) continuous laminae, (d) irre geometry.

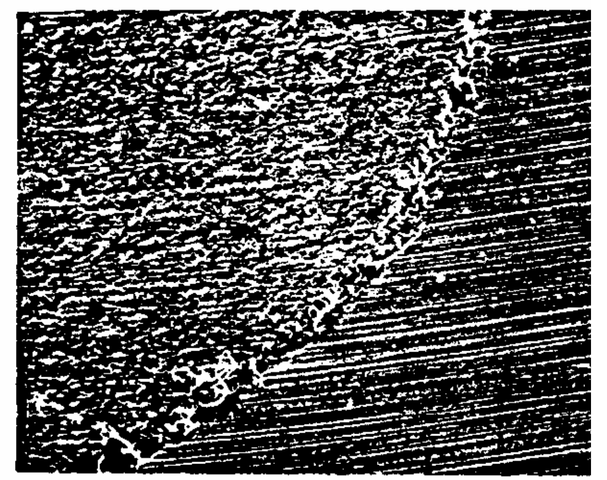

Figure 9 Scanning electron micrograph (× 100) sho marginal gap produced by difference in thermal expa coefficients of dental filling material and tooth subs (courtesy Dr W. Finger).

JOURNAL OF MATERIALS SCIENCE 17 (1982) 2337–2342

Determination of the thermal conductivity and diffusivity of thin fibres by the composite method

J. J. BRENNAN
United Technologies Research Center, East-Hartford, CT 06108, USA

L. D. BENTSEN, D. P. H. HASSELMAN
Department of Materials Engineering, Virginia Polytechnic Institute and State University, Blacksburg, VA 24061, USA

It is suggested that the thermal conductivity of very fine fibres can be evaluated indirectly with the aid of composite theory using the experimental data for the heat transport properties of an appropriate composite which contains the fibres. The feasibility of this approach was investigated by determining the thermal conductivity and diffusivity of fibres of amorphous silicon carbide from 25° C to 1000° C contained within a lithium aluminosilicate glass-ceramic using the laser-flash technique for measurement of the thermal diffusivity of the composite. Due to the amorphous nature of the fibres, values for their thermal conductivity and diffusivity were found to be far less than the corresponding data for crystalline silicon carbide. The positive temperature dependence of the thermal conductivity, coupled with the independent observation of an increase in thermal conductivity with specimen thickness, suggests that radiative heat transfer makes a significant contribution to the total heat transferred. A number of advantages and limitations of the composite method for the evaluation of thermal transport properties of fibres are discussed.

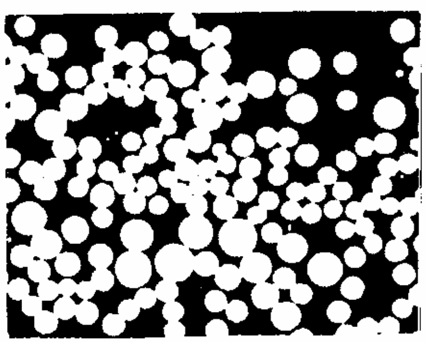

Figure 1 Optical micrograph of 0/90° composite of lithium aluminosilicate glass-ceramic with 45 vol% amorphous silicon carbide fibres.

2.3. Evaluation of the thermal conductivity and diffusivity of the fibres from composite theory

For heat-flow parallel to uniaxially aligned fibres, the thermal conductivity, K_c, of a composite is

$$K_c = K_m V_m + K_p V_p, \quad (1)$$

where K is the thermal conductivity, V is the volume-fraction and the subscripts c, m and p, refer to the composite, matrix and fibres, respectively.

For heat-flow perpendicular to the fibre direction, the thermal conductivity, as derived by Bruggeman [7], can be written

$$\left(\frac{K_m - K_c}{K_m + K_c}\right) V_m = \left(\frac{K_c - K_p}{K_c + K_p}\right) V_p. \quad (2)$$

From the measured value of the thermal diffusivity, the corresponding value of the thermal conductivity, K, can be calculated from

$$K = \kappa \rho c, \quad (3)$$

where κ is the thermal diffusivity, ρ is density and c is the specific heat. The specific heat of the composite can be calculated from the measured values for the specific heat of the fibres and the matrix by means of the rule of mixtures. Substitution of the values for the thermal conductivity of the matrix and the composite into Equation 1 or 2 permits calculations of the thermal conductivity of the fibres. The thermal diffusivity may then be determined using Equation 3.

7. D. A. G. BRUGGEMAN, *Annal. Physik* 24 (1935) 636.

J. Am. Ceram. Soc., 74 [7] 1631–34 (1991)

Role of Interfacial Debonding and Matrix Cracking in the Effective Thermal Diffusivity of Alumina-Fiber-Reinforced ıemical-Vapor-Infiltrated Silicon Carbide Matrix Composites

D. P. H. Hasselman* and A. Venkateswaran*

Department of Materials Engineering, Virginia Polytechnic Institute and State University, Blacksburg, Virginia 24061

H. Tawil

Societe Europeenne de Propulsion, Les Cinq Chemins-Le Haillan, F 33165 Saint Medard en Jalles Cedex, France

thermal diffusivity of a biaxial weave alumina-fiber-forced chemical-vapor-deposited (CVD) SiC composite ɛed to 1500°C, which is above the manufacturing tempera-, was found to exhibit an increase for heat flow parallel ıe fiber plane, whereas a decrease was observed perpen-ılar to the fiber plane. The increase parallel to the fiber ıe was thought to be due to the annealing of the fibers matrix. The decrease perpendicular to the fiber plane found to be the result of interfacial debonding and rix cracking within the plane of the fibers. [Key words: posites, fiber reinforcement, chemical vapor deposition, rmal diffusivity, cracking.]

I. Introduction

ᴵERAMIC matrix composites offer considerable advan-tage over monolithic single-phase ceramics for high-ıperature applications, in view of their enhanced fracture ghness, noncatastrophic failure mode, and increased rmal shock resistance. From the perspective of thermal ılation, temperature control, and energy conservation, ɔrmation on the variables which control the effective ther-l conductivity of ceramic matrix composites is critical for poses of design, materials selection, and performance pre-tion of high-temperature structures and components.

II. Experimental Procedure and Results

Figure 1 shows a SEM micrograph of a polished cross sec-n perpendicular to the fiber direction prior to thermal ɔperty measurement. The fiber volume fraction was ap-ɔximately 42%. The presence of a few pores within the SiC trix indicates that the infiltration process was nearly fully nplete.

Comparison of the data of Figs. 7 and 8 suggests that heating to 1500°C has introduced a structural change of a type such that the ambient gaseous atmosphere affects only heat flow transverse to the fiber direction.

This micrograph clearly indicates the existence of crack formation coupled with interfacial separation within the plane of the fibers. Because cracks do not affect heat conduction parallel to the fiber plane,[18] only the effective thermal conductivity transverse to the plane of the cracks, i.e., transverse to the fiber plane, is expected to be affected, in agreement with the data shown in Figs. 7 and 8. SEM fractographs of samples heated to 1500°C were similar to the one shown in Fig. 2, again showing that crack propagation occurred preferentially along the fiber–matrix interface.

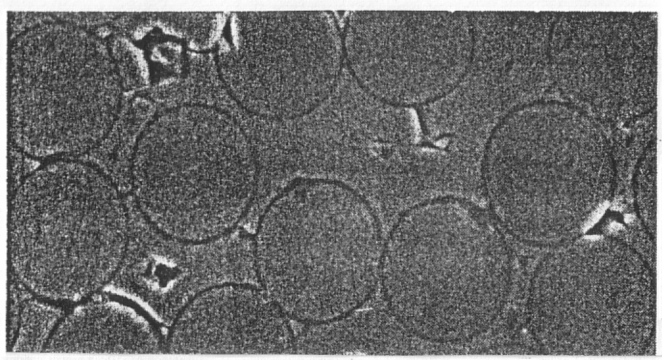

Fig. 9. SEM micrograph of polished section of alumina-fiber-reinforced CVD SiC matrix composite heated to 1500°C in nitrogen, showing evidence of interfacial debonding and matrix cracking.

It is suggested that the matrix cracking and interfac debonding shown in Fig. 9 are related to the differences the coefficient of thermal expansion which for the alumi exceeds the corresponding value for the silicon carbide.

The resulting preferred cra orientation will primarily affect the thermal diffusivity tra verse to the fiber plane.

This mechanism is offered as an explanation for the lo value for the thermal diffusivity in vacuum than in nitro or helium, as shown in Fig. 8. Furthermore, it also prese proof that interfacial and matrix cracks can act as insulat especially under vacuum. Indirect support for the above planations is provided by the data of Eckel and Bradt,[19] v observed a hysteresis in the thermal expansion behavio composites similar to those of the present study, which also attributed to interfacial debonding due to the ther expansion mismatch.

The interfacial spacing and the matrix crack opening placement is such that the gaseous heat transfer is in the called "molecular regime," in which the mean free between collisions of the gaseous species with one anoth much larger than the gap or crack width.[20]

As a final general remark, the results of this reinforce findings of earlier studies[15,17] that the measurement of heat conduction behavior of solids in different gaseous e ronments can be used as a test for microstructural damag nondestructive means.

URNAL OF THERMOPHYSICS AND HEAT TRANSFER
ol. 15, No. 1, January–March 2001

Effective Thermal Conductivity and Thermal Contact Conductance of Graphite Fiber Composites

S. R. Mirmira,* M. C. Jackson,† and L. S. Fletcher‡
Texas A&M University, College Station, Texas 77843-3123

The transverse and longitudinal effective thermal conductivity and contact conductance of discontinuous and misoriented graphite fiber-reinforced composites has been studied over a range of temperatures (20–200°C) and pressures (172–1720 kPa). Three different fiber types (DKE X, DKA X, and K22XX) and three fiber volume fractions (55, 65, and 75%) in a cyanate ester matrix were studied. The addition of fibers to the matrix resulted in an increase in effective thermal conductivity, but appears to level off at fiber volume fractions of 65%. Furthermore, the effective thermal conductivity in the longitudinal direction was significantly greater than in the transverse direction and was more dependent on temperature. These data were used to develop an equation relating the thermal contact conductance to the harmonic mean thermal conductivity of the fiber and matrix material, fiber volume fraction, sample thickness, and microhardness.

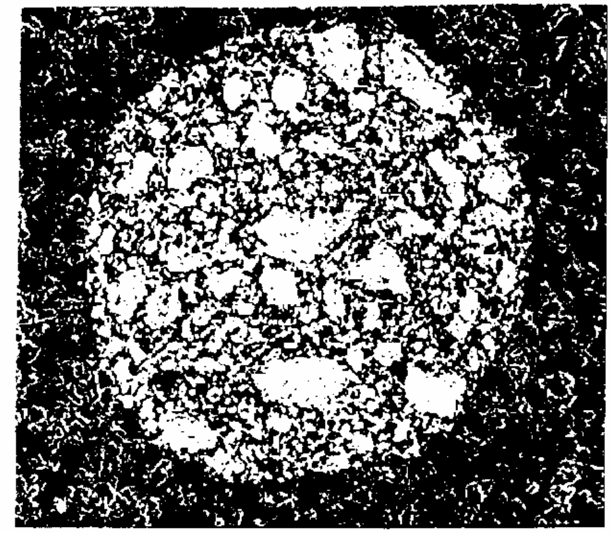

Figure 4.10. Magnified cross section of K22 XX fiber exhibiting a definite texture.

EFFECTIVE THERMAL CONDUCTIVITY OF FIBROUS COMPOSITES:

EXPERIMENTAL AND ANALYTICAL STUDY

A Dissertation

by

SRINIVAS RANGARAO MIRMIRA

Submitted to the Office of Graduate Studies of
Texas A&M University
in partial fulfillment of the requirements for the degree of

DOCTOR OF PHILOSOPHY

December 1999

Figure 4.12. K22 XX ($V_f = 62\%$) fiber indicating fiber splinters and a void between the fiber and matrix.

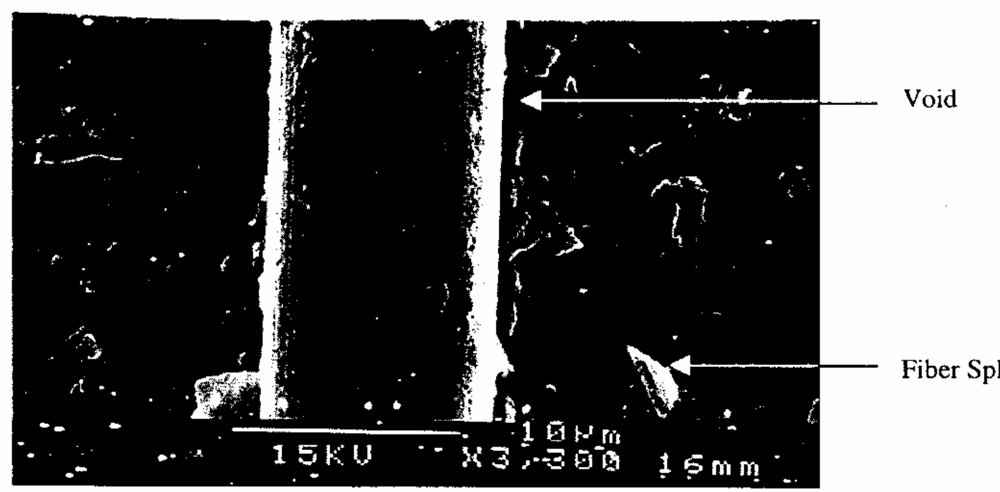

Table 1 Theoretical models for effective thermal conductivity of graphite composites

hor	Expression for effective thermal conductivity	Comments
leigh[6]	$k_e/k_m = 2V_f/\{[(1+k_f/k_m)/(1-k_f/k_m)] + V_f - [(1-k_f/k_m)3V_f^4/(1+k_f/k_m)\pi^4](0.03235\pi^4)^2\}$	Circular filament in a square lattice Transverse effective thermal conductivity Does not account for interfacial thermal resistance between fiber and matrix
rens[8]	$k_e = k_m\left[\frac{(k_f/k_m+1)+V_f(k_f/k_m-1)}{(k_f/k_m+1)-V_f(k_f/k_m-1)}\right]$	Transverse effective thermal conductivity Circular filament in a square lattice Does not account for fiber orientation or interfacial thermal resistance
shin[9]	$K_e^+ = k_f\left[1+V_m\Big/\left(\frac{k_m}{k_f-k_m}+\frac{V_m}{3}\right)\right]$ $K_e^- = k_m\left[1+V_f\Big/\left(\frac{k_m}{k_f-k_m}+\frac{V_m}{3}\right)\right]$	Bounded solution for transverse effective thermal conductivity Arbitrary phase geometry
ng and Vachon[10]	$k_e = k_m\Big/\left(1-\sqrt{3V_f/2}\right)$	Parabolic, random distribution of fibers Only accurate for $V_f < 66.7$
chelor and O'Brien[11]	$k_e = 4.0k_m \log_e(k_f/k_m)$	Random array of uniform spherical particles Accounts for point contact among particles Applicable for $k_f/k_m \gg 1$
shin[12]	$k_e^+ = k_f\frac{k_f v_f + k_m(1+V_m)}{k_f(1+V_m)+k_m V_f}, \quad k_e^- = k_m\frac{k_m v_m + k_f(1+V_f)}{k_m(1+V_f)+k_f V_m}$	Fibers isotropic along their length only Lower bound equivalent to that of Behrens[8]
mura and Chou[13]	$k_e^+ = \frac{(V_m k_m + V_f k_f)^2 + k_m k_f}{(k_m+k_f)}, \quad k_e^- = \frac{(k_m+k_f)k_m k_f}{(V_f k_m + V_m k_f)^2 + k_m k_f}$	Transverse effective thermal conductivity Fibers isotropic along their length only Fiber has ellipsoidal symmetry Simplified formula for an aligned long fiber composite
amis[14]	$k_e = \left(1-\sqrt{V_f}\right)k_m + \frac{k_m\sqrt{V_f}}{1-\sqrt{V_f}(1-k_m/k_f)}$	Long, continuous, circular fibers in square array Unidirectional fibers Transverse effective thermal conductivity
ta and Taya[15]	$k_e = k_m\left[1+V_f\Big/\left(\frac{1-V_f}{3}+\frac{k_m}{k_f-k_m}\right)\right]$	Three-dimensional misoriented short fibers Fibers are not in contact Simplifies to Hashin's[9] lower bound
uso and Chamis[16]	$k_e = (1-\sqrt{V_f})k_m + \frac{k_m\sqrt{V_f}}{1-\sqrt{V_f}(1-V_m/V_f)}$	Transverse effective thermal conductivity Unidirectional continuous fibers Fibers arranged in a square cell
ttram and Taylor[17]	$\frac{k_e}{k_m} = \left(\left\{\sqrt{\left[\left(1-\frac{V_f}{1-V_p}\right)^2\left(\frac{k_f}{k_m}-1\right)^2+\frac{4k_f}{k_m}\right]} - \left(1-\frac{V_f}{1-V_p}\right)\left(\frac{k_f}{k_m}-1\right)\right\}^2\Big/4\right)(1-V_p)\left(\frac{X+1}{x}\right)$ $x = 2$ for spheres $= 1$ for cylinders perpendicular to heat flow	Accounts for shape of discontinuous phase. Model does not account for interface resistance and spacing of the fibers.
sselman and Johnson[18]	$k_e = k_m\left\{\left[2V_f\left(\frac{k_f}{k_m}-\frac{k_f}{rh_i}-1\right)+\frac{k_f}{k_m}+2\frac{k_f}{rh_i}+2\right]\Big/\left[V_f\left(1-\frac{k_f}{k_m}+\frac{k_f}{rh_i}\right)+\frac{k_f}{k_m}+2\frac{k_f}{rh_i}+2\right]\right\}$	Randomly dispersed spherical inclusions with a coating Dilute fiber volume fractions No interaction between fiber and matrix

Based on this review, it appears that modeling the effective thermal conductivity of fiber composites should account for the geometrical arrangement of the fibers, the dimensions of the fibers, the fiber volume fraction, and thermal conductivity of the fiber and matrix. The model should also account for the interfacial thermal resistance between the fiber and the matrix and the possibility of transversely anisotropic fibers.

Experimental Program

To provide additional experimental data on the effective thermal conductivity and thermal contact conductance of discontinuous graphite fiber composites, under controlled conditions, an experimental program was undertaken. The following sections describe the materials selected, the test facility, experimental procedure, and the uncertainty associated with results.

To avoid convection losses, the entire test facility was housed in a vacuum of 1×10^{-5} torr maintained by an oil diffusion pump backed by a two-stage rotary pump. Further, radiative losses from the fluxmeters and samples were reduced by placing a segmented radiation shield around the vertical test column.

Conclusions

On one hand, the transverse effective thermal conductivity of the composites was highest for fiber volume fractions of 65%, above which the increased interfacial thermal resistance between the fiber and matrix negated any benefit due to greater fiber volume. On the other hand, the longitudinal effective thermal conductivity increased for higher fiber volume fractions. The longitudinal thermal conductivity was approximately one order of magnitude greater than the transverse. Furthermore, the effective thermal conductivity of the composite did not vary significantly over the selected temperature range.

Considering the importance of the interfacial thermal resistance between the fiber and the matrix, it is recommended that a fundamental experiment be conducted (ideally with known number of fibers) to quantify this value as a function of material properties. It is also recommended that the effect of cryogenic temperatures on the thermal conductivity be examined and a larger range of fiber volume fractions be tested. Further, it is apparent that the present models do not accurately predict the thermal conductivity of graphite composites. It would be beneficial to develop a model that accounts for the various influencing parameters, including the interfacial thermal resistance between the fibers and the matrix. Electron microscopy studies would reveal the nature of bonding between the fibers and the matrix, as well as the presence of voids.

Materials Science and Technology August 2003 Vol. 19

lumerical simulation of thermal conductivity of IMCs: effect of thermal interface resistance

Duschlbauer, H. J. Böhm and H. E. Pettermann

e thermal conductivity of metal matrix composites is investigated by computational simulations, in which the ect of a thermal barrier resistance between the constituent phases is explicitly taken into account. A numerical it cell approach, which is based on the finite element method, an analytical mean field method of the Mori–naka type and bounding techniques are employed. To predict the effective conductivities of fibre composites two ferent types of unit cell are utilised for the numerical studies. Two dimensional unit cells are developed which ow for investigations of aligned, continuous fibre reinforced composites while three dimensional unit cells are ıployed to study a large variety of different arrangements of non-staggered and staggered aligned short fibres. In : case of short fibres the thermal barrier resistances of the end faces and of the cylindrical surfaces are modelled lependently, which allows one to study both their individual and their combined influences on the overall haviour. Results are presented for carbon fibre/copper composites and their overall thermal conductivities are ·estigated in terms of interfacial thermal barriers and microtopologies. MST/5341

troduction

ɜtal matrix composites (MMCs) are widely used in ctronic packaging applications, because of the possibility tailoring the properties of the composite. The coefficient thermal expansion (CTE) and thermal conductivity are : two most important design parameters.

Because of copper's non-reactivity with carbon, a draw-ck of carbon–copper composites is the poor matrix/fibre :erface, which severely reduces the effective heat flow ssing through the interface.

Due to different morphologies of carbon fibres' end faces l cylindrical surfaces (side faces) but also due to breaking carbon fibres (e.g. during the hot pressing process of coated fibres, leaving fibres with coated side faces and n-coated end faces), high risk and low risk areas of tential thermal interface degradation are created. It is an n of the present investigation to determine the effects of :erface failure on the effective conductivity.

Numerous models have been published for predicting the effective transport properties of heterogeneous media. The majority of the analytical estimates have been based on the equivalent inclusion method dealing with inclusions of ellipsoidal shape. In this basic form these models assume ideal thermal contact between the constituents,[3–6] and extensions for modelling coated inclusions have been reported.[7,8] The implementation of non-ideal thermal interfaces where the temperature field is not continuous at constituent faces[9,10] represents another group of extended models.

The interfacial thermal barrier was modelled as a layer of small (but finite) thickness and poor conductivity, i.e. introducing a third phase.

In the present work, numerical unit cell studies focus on aligned CFRCs and aligned, short fibre reinforced composites (SFRCs). In the case of CFRCs, regular fibre arrangements as well as random fibre arrangements are investigated. SFRCs are studied with respect to the influence of axial fibre offset and the degree of stagger on the effective conductivity. For both CFRCs and SFRCs the influence of thermal barriers at the fibre/matrix interfaces on the effective conductivity is investigated by means of appropriate thermal interface elements. For the analytical studies a Mori–Tanaka type approach for coated inclusions is used, which is applicable to the case of thermal interfacial resistances as well.

Thermal interface barrier

An interfacial thermal barrier between matrix and fibr arise because of poor mechanical contact, the preser impurities at the interface or debonded regions.

Unlike earlier work,[11,12] where the thermal inter barrier was implemented into FEM via an interphase c conductivity, in the present work the thermal inter barrier is implemented as an interface within the un approach. Specific thermal contact surface element employed at the constituent interfaces.

composite with fixed volume fraction, skin con inclusion shape and orientation, containing large inclu exhibits a higher effective conductivity than would t case for smaller inclusions due to the fact that the ra inclusion surface area (i.e. the interfacial area) to vo decreases as the inclusion size increases.[10]

Unit cell approach

The unit cell approach describes the macroscale and m scale behaviour of inhomogeneous materials by stud model materials that have idealised periodic micros tures.

(a)

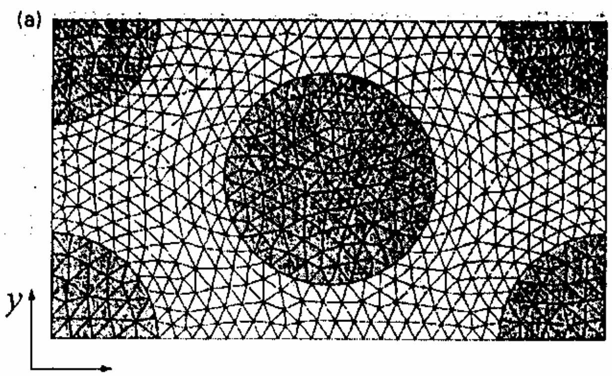

1 Two dimensional unit cells for periodic arrangemen (rectangular) of aligned continuously reinforced composites: fibre volume fraction $\xi=0{\cdot}4$

NIT CELLS FOR CONTINUOUSLY FIBRE EINFORCED COMPOSITES

Clearly these regular rangements do not fully represent 'real' composites. nproved models can be obtained with multifibre unit cells which fibre positions are selected randomly or taken from icrographs. In the present study a unit cell with seudorandom fibre positions is used, which is based on 1 arrangement used earlier[21]

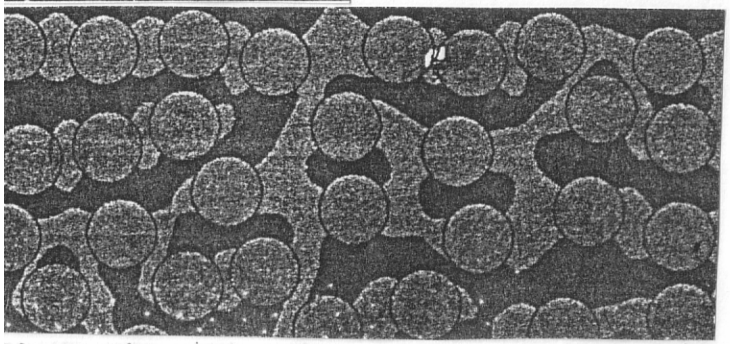

If some microtopology shows a set of parallel symmetry anes, these planes have special properties.

Symmetry BCs are very useful for describing simple, gular microgeometries, but they are less suited to model ndom arrangements. On the one hand a random rangement suitable for symmetry BCs is only pseudoran- om as the fibres may either not touch a face or must be sected by one or more faces, and on the other hand it is sumed that the heat flux orthogonal to the applied adient is zero, which always automatically sets the fective conductivity k^*_{xy} to zero (compare equation (8)). nly for sufficiently large random unit cells with almost otropic effective conductivities can this effect be neglected.

For the numerical and analytical studies, conductivities e chosen to be independent of the temperature. Never- eless the studies can be readily extended to the case of mperature dependent conductivities by repeatedly run- ng the calculations with the appropriate constituent nductivities corresponding to a particular temperature. ith this procedure the temperature dependent thermal mposite behaviour is predicted for discrete temperatures r small temperature differences within the unit cell.

It should be noted that only stationary fields are con- lered, i.e. initial temperature distributions, specific heat and nstituent densities do not influence the effective conduct- ties of the composite. Investigations of transient processes em feasible by means of appropriate FEM models, yielding ne-dependent and local effective conductivities.

UNIT CELLS FOR STAGGERED SHORT FIBRE COMPOSITES

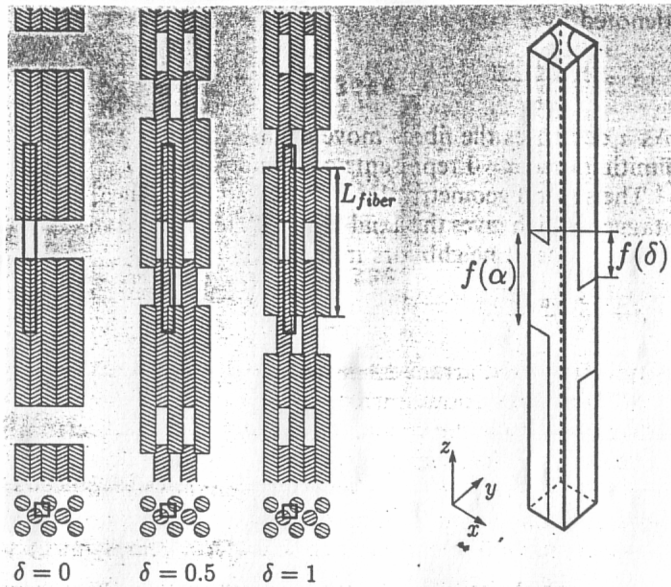

3 *a* different staggered and non-staggered arrangements of aligned short fibres (aspect ratio = 10) for axial fibre offset $\alpha = 0{\cdot}25$; *b* geometry parameters δ and α describe degree of staggering and axial fibre offset

EFFECTIVE CONDUCTIVITIES

For the numerical and analytical studies, conductivities are chosen to be independent of the temperature. Nevertheless the studies can be readily extended to the case of temperature dependent conductivities by repeatedly running the calculations with the appropriate constituent conductivities corresponding to a particular temperature. With this procedure the temperature dependent thermal composite behaviour is predicted for discrete temperatures for small temperature differences within the unit cell.

It should be noted that only stationary fields are considered, i.e. initial temperature distributions, specific heat and constituent densities do not influence the effective conductivities of the composite. Investigations of transient processes seem feasible by means of appropriate FEM models, yielding time-dependent and local effective conductivities.

Results and discussion

As an example carbon/copper composites are chosen, w are produced by hot pressing; matrix and fibre material are listed in Table 1. The conductivity of the isot copper matrix is approximately 10% less than theoretical conductivity of 99% copper, due to contar tion and pores left after the hot pressing process.

All calculations are carried out for carbon/copper posites with a fibre volume fraction $\xi = 0{\cdot}4$. The fibr SFRCs are modelled as cylinders with an aspect ratio c

Unit cell calculations are carried out with the element program ANSYS 5·7.[23] Two dimensional unit are meshed with six node triangular elements, dimensional unit cells are meshed with 10 node tetrah elements. The thermal interface was modelled with a priate contact/target surface elements, which are overla the constituent interfaces, allowing for non-conf meshes at the interface.

Thermal barrier interface The influence of the th interface is studied for a square and a rectangular $a_{\square} = 0{\cdot}6$) arrangement. The interface conduc ($\beta \cdot r_{fibre}$, r_{fibre} being the fibre radius) is varied from to 10^7 W m^{-1} K^{-1}, covering the range from per insulating interfaces to perfectly conducting interface

Failure of the end face interfaces

The influence of decohesion or lack of contact c interfaces at the fibres' end faces, i.e. perfectly insu interfaces, is also investigated. The effective axial ductivities are reduced severely while the effective tran conductivity is less affected (Table 3, Fig. 6).

The effective transverse cond ity is reduced only slightly due to the presence of the th barrier at the end faces (for all arrangements the redu is less than 0·1%).

The setup of the microarrangements was highly idea as perfectly periodic arrangements are not fully real Nevertheless useful insight and information on the i dependence of the topological input parameters was ga

When compared to three dimensional unit cells randomly oriented fibres, the cells employed for ali fibres can be set up relatively easily to meet high volume fractions requirements, and they are not demanding with regard to computational requirements present approach can easily be applied to other m topologies. Extensions to fully coupled thermomecha investigations of high volume fraction, three dimens unit cells with randomly oriented fibres and with consi tion of load dependent progressive failure of the inter are feasible.

INTRODUÇÃO (cont.)

- Características dos materiais compósitos
  - ➢ Presença de grande número de partículas ou fibras
  - ➢ Escalas de comprimento bastante díspares
    - ✓ MACROESCALA: dimensão física do compósito (cm -> m)
    - ✓ MesoEscala: dimensão característica da microestrutura do compósito (μm –> mm)
    - ✓ microescala: dimensão característica das partículas/fibras (μm)

- Condução de calor em compósitos
  - ➢ Problema de transporte em meio com múltiplas escalas
  - ➢ Difícil aplicação direta de métodos analíticos e numéricos convencionais
  - ➢ Difícil determinação do campo local de temperatura
  - ➢ Comportamento térmico macroscópico destes materiais pode ser descrito uma vez conhecida a condutividade térmica efetiva

BREVE REVISÃO DA LITERATURA

- MÉTODOS DE DETERMINAÇÃO DE LIMITES
  (Torquato & Rintoul, 1995; Torquato, 1991; Nomura & Chou, 1980)

  - Determinação rigorosa de limites inferiores e superiores
  - Funções de correlação espacial para a microestrutura
  - Raramente concordam bem com dados experimentais (principalmente para razão de condutividades elevada)

- MÉTODOS ANALÍTICOS E SEMI-ANALÍTICOS
  (Cheng & Torquato, 1997; Furmañski, 1991; Sangani & Yao, 1988; Sangani & Acrivos, 1983; Perrins et al., 1979)

  - Geometrias simples (e.g., esferas e elipsóides)
  - Limite de diluição (pequenas frações de volume da fase dispersa)
  - Distribuições randômicas das partículas

BREVE REVISÃO DA LITERATURA (cont.)

- ABORDAGENS FENOMENOLÓGICAS
  (Dunn et al., 1993; Hasselman et al., 1993; Benveniste et al., 1990; Hatta & Taya, 1986; Hashin, 1968)

  - Hipóteses heurísticas simplificadoras: conceito do campo médio de MORI-TANAKA e método da inclusão equivalente de ESHELBY
  - Distribuições de orientação e razão de aspecto de fibras
  - A maioria despreza as interações entre fibras vizinhas
  - A maioria adota a hipótese de contato térmico perfeito
  - Resistência térmica interfacial: arranjos 2-D de fibras cilíndricas de comprimento infinito
  - Expressões para a condutividade térmica efetiva “válidas” para pequenas e médias frações de volume da fase dispersa

BREVE REVISÃO DA LITERATURA (cont.)

- COMPUTACIONAL
  (Duschlbauer et al., 2003; Matt & Cruz, 2002; Matt & Cruz, 2001; Rocha & Cruz, 2001; Veyret et al., 1993; Ingber et al., 1994; James & Keen, 1985)

  - Flexibilidade para incorporar efeitos geométricos e físicos
  - Maioria restrita a microestruturas 2-D
  - Microestrutura tem que ser prescrita
  - MEF, MDF, MEC

- EXPERIMENTAL
  (Jiajun & Xiao-Su, 2004; Garnier et al., 2002; Mirmira & Fletcher, 2001; Mirmira, 1999)

  - Física completa
  - Crítica à maioria das metodologias existentes por superestimarem a condutividade térmica efetiva de compósitos
  - Estimativa da resistência térmica interfacial
  - Estimativa da fração volumétrica de poros na matriz
  - Informações a respeito da forma e orientação das fibras
  - Comparação difícil com resultados teóricos/numéricos

CONDUÇÃO DE CALOR EM COMPÓSITOS

- Descrição física

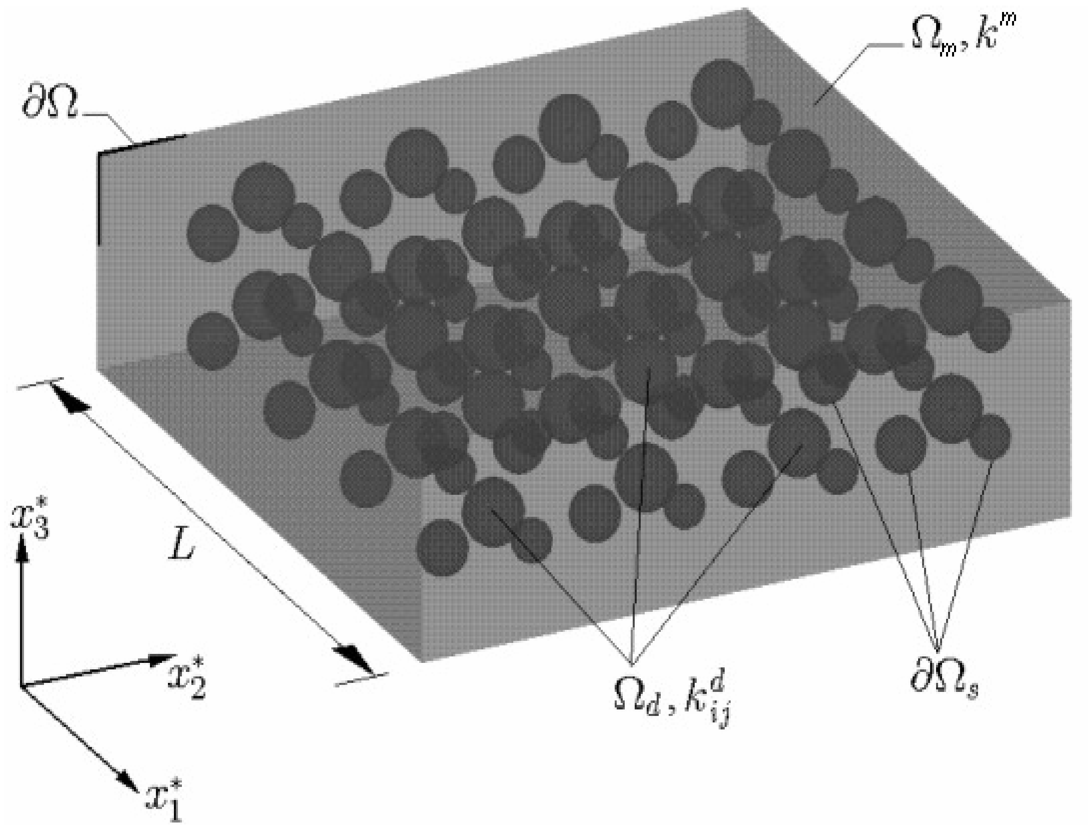

compósito com microestrutura 3-D

CONDUÇÃO DE CALOR EM COMPÓSITOS (cont.)

- Formulação matemática (forma forte dimensional)

$$
\begin{aligned}
-\frac{\partial}{\partial x_i^*}\left(k^m \frac{\partial T^m}{\partial x_i^*}\right) &= \dot{g}_m \text{ em } \Omega_m \\
-\frac{\partial}{\partial x_i^*}\left(k_{ij}^d \frac{\partial T^d}{\partial x_j^*}\right) &= \dot{g}_d \text{ em } \Omega_d
\end{aligned}
$$

$$
\begin{aligned}
-k^m \frac{\partial T^m}{\partial x_i^*} n_i^m &= -k_{ij}^d \frac{\partial T^d}{\partial x_j^*} n_i^m \text{ em } \partial\Omega_s \\
-k^m \frac{\partial T^m}{\partial x_i^*} n_i^m &= h_s \left(T^m - T^d\right) \text{ em } \partial\Omega_s
\end{aligned}
$$

CONDUÇÃO DE CALOR EM COMPÓSITOS (cont.)

- Formulação matemática (forma forte adimensional)

$$-\frac{\partial}{\partial y_i}\left(\frac{\partial \theta^m}{\partial y_i}\right) = \frac{\dot{g}_m\,\lambda^2}{k^m\,\Delta T} \text{ em } \Omega_m$$

$$-\frac{\partial}{\partial y_i}\left(\kappa_{ij}\,\frac{\partial \theta^d}{\partial y_j}\right) = \frac{\dot{g}_d\,\lambda^2}{k^m\,\Delta T} \text{ em } \Omega_d$$

$$-\frac{\partial \theta^m}{\partial y_i}\,n_i^m = -\kappa_{ij}\,\frac{\partial \theta^d}{\partial y_j}\,n_i^m \text{ em } \partial\Omega_s$$

$$-\frac{\partial \theta^m}{\partial y_i}\,n_i^m = \boxed{\frac{h_s\,\lambda}{k^m}}\left(\theta^m - \theta^d\right) \text{ em } \partial\Omega_s$$

magnitude da resistência térmica interfacial

$$\mathbf{y} \equiv \frac{\mathbf{x}^*}{\lambda}$$

$$\theta^m(\mathbf{x}^*) \equiv \frac{T^m(\mathbf{x}^*)}{\Delta T}$$

$$\theta^d(\mathbf{x}^*) \equiv \frac{T^d(\mathbf{x}^*)}{\Delta T}$$

$$\kappa_{ij} \equiv \frac{k_{ij}^d}{k^m}$$

$$G_m \equiv \frac{\dot{g}_m\lambda^2}{k^m\Delta T}$$

$$G_d \equiv \frac{\dot{g}_d\lambda^2}{k^m\Delta T}$$

$$\mathrm{Bi} \equiv \frac{h_s\,\lambda}{k^m}$$

CONDUÇÃO DE CALOR EM COMPÓSITOS (cont.)

- Formulação matemática (forma fraca)
  - ➢ Vantagens da forma fraca
    - ✓ Condição de contorno de continuidade do fluxo de calor na interface naturalmente imposta ($\Rightarrow$ facilidade para incorporação de vazios)
    - ✓ Compatibilização com o método dos elementos finitos
  - ➢ Definição dos espaços de funções

$$X'(\Omega) \;=\; \{w \in H^1(\Omega) | w_{|\Omega_c \subset \Omega} = w^c, w_{|\Omega_d \subset \Omega} = w^d, [w]_{\partial\Omega_s} = s \in I\!R\}$$

$$X(\Omega) = X'(\Omega) \cap H_0^1(\Omega) \qquad\qquad H_0^1(\Omega) \subset H^1(\Omega)$$

CONDUÇÃO DE CALOR EM COMPÓSITOS (cont.)

- Formulação matemática (forma fraca)
  - Enunciado

dados $\zeta_{ij}(\mathbf{y})$, Bi e $G(\mathbf{y})$, encontrar $\theta(\mathbf{y}) \in X'(\Omega)$ tal que

$$\int_{\Omega} \zeta_{ij}(\mathbf{y}) \, \frac{\partial \theta}{\partial y_j} \, \frac{\partial v}{\partial y_i} \, d\mathbf{y} + \int_{\partial \Omega_s} \mathrm{Bi} \, [v]_{\partial \Omega_s} [\theta]_{\partial \Omega_s} \, ds = \int_{\Omega} v \, G \, d\mathbf{y} \quad \forall v \in X(\Omega)$$

$$v, \theta, \zeta_{ij}(\mathbf{y}), G = \begin{cases} v^m, \theta^m, \delta_{ij}, G_m & \text{em} \quad \Omega_m \subset \Omega \\ v^d, \theta^d, \kappa_{ij}, G_d & \text{em} \quad \Omega_d \subset \Omega. \end{cases}$$

CONDUÇÃO DE CALOR EM COMPÓSITOS (cont.)

- TEORIA DA HOMOGENEIZAÇÃO
  (Milton, 2002; Auriault & Ene, 1994; Auriault, 1991; Bakhvalov & Panasenko, 1989; Bensoussan et al., 1978; Babuska, 1975)

  - Técnica matemática rigorosa

  - Aplicada a uma variedade de fenômenos de transporte em meios heterogêneos

  - Comportamento da solução no limite em que a razão de escalas de comprimento tende a zero

  - Transforma o problema de transporte definido no meio heterogêneo original em dois problemas mais fáceis de serem resolvidos
    - ✓ Problema homogeneizado
    - ✓ Problema da célula

CONDUÇÃO DE CALOR EM COMPÓSITOS (cont.)

- TEORIA DA HOMOGENEIZAÇÃO
  (Milton, 2002; Auriault, 1991; Bakhvalov & Panasenko, 1989; Bensoussan et al., 1978)

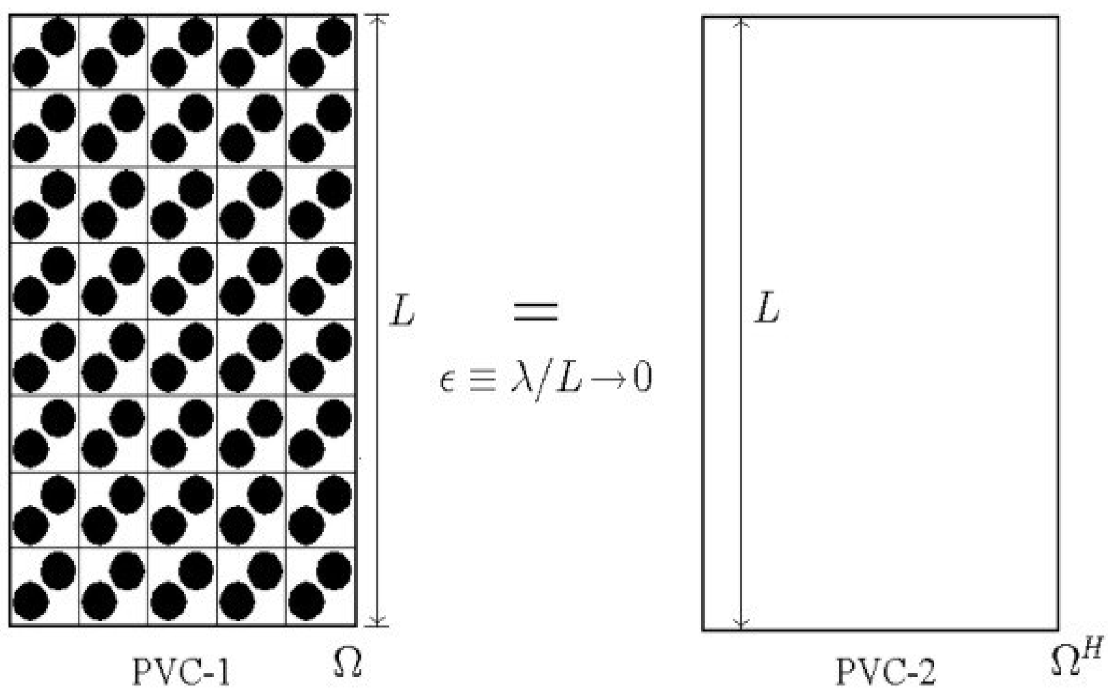

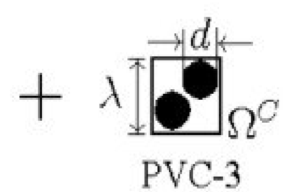

célula representativa da microestrutura (RVE)

meio heterogêneo

meio homogêneo

CONDUÇÃO DE CALOR EM COMPÓSITOS (cont.)

- TEORIA DA HOMOGENEIZAÇÃO
  - Técnica das expansões assintóticas utilizando múltiplas escalas
  - Técnica apropriada para problemas de transporte definidos em meios estatisticamente homogêneos que apresentam uma separação natural de escalas
  - Solução é escrita em função de duas variáveis
    - ✓ Variável rápida (coordenada da mesoescala)
    - ✓ Variável lenta (coordenada da macroescala)

$$\epsilon \equiv \lambda / L \ll 1$$

$$\begin{aligned} \theta(\mathbf{x},\mathbf{y}) &= \theta_0(\mathbf{x},\mathbf{y}) + \epsilon\,\theta_1(\mathbf{x},\mathbf{y}) + \epsilon^2\,\theta_2(\mathbf{x},\mathbf{y}) + \ldots \\ v(\mathbf{x},\mathbf{y}) &= v_0(\mathbf{x},\mathbf{y}) + \epsilon\,v_1(\mathbf{x},\mathbf{y}) + \epsilon^2\,v_2(\mathbf{x},\mathbf{y}) + \ldots \end{aligned}$$

$$\mathbf{y} \equiv \mathbf{x}^*/\lambda$$

(variável rápida)

$$\mathbf{x} \equiv \mathbf{x}^*/L = \epsilon\,\mathbf{y}$$

(variável lenta)

CONDUÇÃO DE CALOR EM COMPÓSITOS (cont.)

- APLICAÇÃO DA TEORIA DA HOMOGENEIZAÇÃO
  - Substituindo as expansões para θ e v na forma fraca...

$$\int_{\Omega} \zeta_{ij} \left(\frac{\partial v_0}{\partial y_i} + \epsilon \frac{\partial v_0}{\partial x_i} + \epsilon \frac{\partial v_1}{\partial y_i} + \epsilon^2 \frac{\partial v_1}{\partial x_i} + \epsilon^2 \frac{\partial v_2}{\partial y_i} \right) \left(\frac{\partial \theta_0}{\partial y_j} + \epsilon \frac{\partial \theta_0}{\partial x_j} + \epsilon \frac{\partial \theta_1}{\partial y_j} + \epsilon^2 \frac{\partial \theta_1}{\partial x_j} + \epsilon^2 \frac{\partial \theta_2}{\partial y_j} \right) d\mathbf{y}$$
$$+ \int_{\partial\Omega_s} \mathrm{Bi} \left[v_0 + \epsilon v_1 + \epsilon^2 v_2 \right]_{\partial\Omega_s} \left[\theta_0 + \epsilon \theta_1 + \epsilon^2 \theta_2 \right]_{\partial\Omega_s} d\mathbf{s}$$

$$= \int_{\Omega} \left(v_0 + \epsilon v_1 + \epsilon^2 v_2 \right) G \, d\mathbf{y} \quad \forall v_0, v_1, v_2 \in X(\Omega)$$

  - Condição de homogeneização: $\theta_0 \neq 0 \quad \Rightarrow \quad G = O(\epsilon^2)$
    (a quantidade de calor gerada internamente no compósito deve ser da mesma ordem de grandeza da quantidade de calor conduzida na macroescala)
  - Cinco modelos para magnitude da resistência térmica interfacial
    (Rocha, 1999; Auriault & Ene, 1994)

$$\mathrm{Bi} = O(\epsilon^a),\ a \in \{-1, 0, 1, 2, 3\} \qquad \text{modelo II } (a = 0)$$

CONDUÇÃO DE CALOR EM COMPÓSITOS (cont.)

- APLICAÇÃO DA TEORIA DA HOMOGENEIZAÇÃO
  - Agrupando potências iguais de ε, obtém-se

$$\left[\theta_0^{\mathrm{II}}\right]_{\partial\Omega_s} = 0$$

$$\frac{\partial \theta_0^{\mathrm{II}}}{\partial y_j} = 0, j = 1, 2, 3$$

$$\int_\Omega \zeta_{ij} \left(\frac{\partial \theta_0^{\mathrm{II}}}{\partial x_j} \frac{\partial v_0^{\mathrm{II}}}{\partial x_i} + \frac{\partial \theta_1^{\mathrm{II}}}{\partial y_j} \frac{\partial v_0^{\mathrm{II}}}{\partial x_i} + \frac{\partial \theta_0^{\mathrm{II}}}{\partial x_j} \frac{\partial v_1^{\mathrm{II}}}{\partial y_i} + \frac{\partial \theta_1^{\mathrm{II}}}{\partial y_j} \frac{\partial v_1^{\mathrm{II}}}{\partial y_i} \right) d\mathbf{y} \quad + \\ + \int_{\partial\Omega_s} \mathrm{Bi} \left[v_1^{\mathrm{II}}\right]_{\partial\Omega_s} \left[\theta_1^{\mathrm{II}}\right]_{\partial\Omega_s} ds \quad = \quad \int_\Omega v_0^{\mathrm{II}}\, G\, d\mathbf{y}$$

$$\forall v_0^{\mathrm{II}}, v_1^{\mathrm{II}} \in X(\Omega)$$

CONDUÇÃO DE CALOR EM COMPÓSITOS (cont.)

- APLICAÇÃO DA TEORIA DA HOMOGENEIZAÇÃO

Escolhendo primeiramente $v_0^{II} = 0$ e depois $v_1^{II} = 0$, obtém-se

$v_0^{II} = 0$

$$\int_\Omega \zeta_{ij} \frac{\partial v_1^{II}}{\partial y_i} \left(\frac{\partial \theta_0^{II}}{\partial x_j} + \frac{\partial \theta_1^{II}}{\partial y_j} \right) d\mathbf{y} + \int_{\partial\Omega_s} \mathrm{Bi} \left[v_1^{II} \right]_{\partial\Omega_s} \left[\theta_1^{II} \right]_{\partial\Omega_s} ds = 0 \quad \forall v_1^{II} \in X(\Omega)$$

$v_1^{II} = 0$

$$\int_\Omega \zeta_{ij} \frac{\partial v_0^{II}}{\partial x_i} \left(\frac{\partial \theta_0^{II}}{\partial x_j} + \frac{\partial \theta_1^{II}}{\partial y_j} \right) d\mathbf{y} = \int_\Omega v_0^{II} G \, d\mathbf{y} \quad \forall v_0^{II} \in X(\Omega)$$

CONDUÇÃO DE CALOR EM COMPÓSITOS (cont.)

- APLICAÇÃO DA TEORIA DA HOMOGENEIZAÇÃO

Propondo a seguinte separação de variáveis para $\theta_1^{II}(\mathbf{x},\mathbf{y})$

$$\theta_1^{II}(\mathbf{x},\mathbf{y}) \;=\; -\chi_p^{II}(\mathbf{y})\,\frac{\partial\theta_0^{II}}{\partial x_p}(\mathbf{x})$$

e aplicando a propriedade de periodicidade para as integrais de volume (Rocha & Cruz, 2001; Auriault, 1991) e de superfície (Rocha & Cruz, 2001)

$$\lim_{\epsilon\to 0}\left(\int_\Omega f(\mathbf{x},\mathbf{y})\;d\mathbf{y} + \int_{\partial\Omega_s} g(\mathbf{x},\mathbf{y})\;ds\right) = \int_\Omega \frac{1}{|\Omega_{pc}|}\left(\int_{\Omega_{pc}} f(\mathbf{x},\mathbf{y})\;d\mathbf{y} + \int_\Gamma g(\mathbf{x},\mathbf{y})\;ds\right)d\mathbf{y}$$

Ω_{pc} Elemento de volume representativo da microestrutura (suposta periódica) ou célula periódica

Γ Porção da interface entre as fases no interior de Ω_{pc}

CONDUÇÃO DE CALOR EM COMPÓSITOS (cont.)

- APLICAÇÃO DA TEORIA DA HOMOGENEIZAÇÃO
  - Problema da célula

$$\int_{\Omega_{pc}} \zeta_{ij} \frac{\partial \chi_p^{\mathrm{II}}}{\partial y_j} \frac{\partial v}{\partial y_i}\, d\mathbf{y} + \int_{\Gamma} \mathrm{Bi}\,[v]_\Gamma \left[\chi_p^{\mathrm{II}}\right]_\Gamma ds = \int_{\Omega_{pc}} \zeta_{ip} \frac{\partial v}{\partial y_i}\, d\mathbf{y} \qquad \forall v \in Y^{\mathrm{II}}(\Omega_{pc})$$

$$Y^{\mathrm{II}}(\Omega_{pc}) = \left\{ w \in H^1_\#(\Omega_{pc}) | w_{|\Omega_{pc,c} \subset \Omega_{pc}} = w^c, w_{|\Omega_{pc,d} \subset \Omega_{pc}} = w^d, [w]_\Gamma = s \in I\!R^* \right\}$$

  - Problema homogeneizado

$$\int_\Omega \left\{ \frac{1}{|\Omega_{pc}|} \int_{\Omega_{pc}} \zeta_{ij} \left(\delta_{jp} - \frac{\partial \chi_p^{\mathrm{II}}}{\partial y_j} \right) d\mathbf{y} \right\} \frac{\partial v_0^{\mathrm{II}}}{\partial x_i} \frac{\partial \theta_0^{\mathrm{II}}}{\partial x_p}\, d\mathbf{y} = \int_\Omega \left(\frac{1}{|\Omega_{pc}|} \int_{\Omega_{pc}} v_0^{\mathrm{II}}\, G\, d\mathbf{y} \right) d\mathbf{y} \quad \forall v_0^{\mathrm{II}} \in X(\Omega)$$

  - Tensor condutividade térmica efetiva

$$\kappa_{pq}^{\epsilon,\mathrm{II}} \equiv \frac{k_{pq}^{\epsilon,\mathrm{II}}}{k^m} = \frac{1}{|\Omega_{pc}|} \int_{\Omega_{pc}} \zeta_{pi} \left(\delta_{iq} - \frac{\partial \chi_q^{\mathrm{II}}}{\partial y_i} \right) d\mathbf{y}$$

MÉTODOS NUMÉRICOS

- MODELOS GEOMÉTRICOS PARA CÉLULA PERIÓDICA
  - Arranjos ordenados de esferas

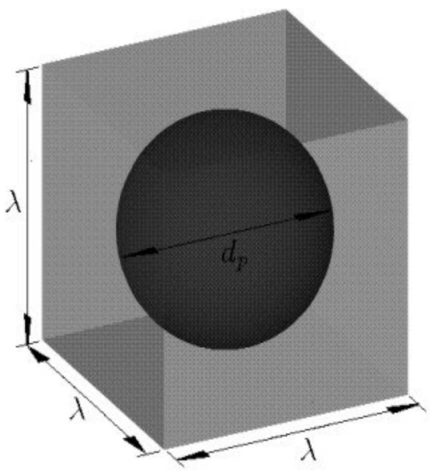

  - Arranjos desordenados de esferas

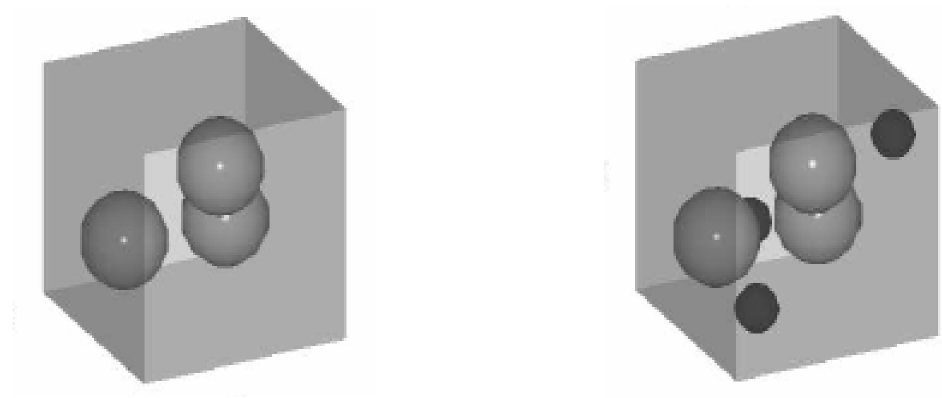

MÉTODOS NUMÉRICOS (cont.)

- MODELOS GEOMÉTRICOS PARA CÉLULA PERIÓDICA
  - Arranjos ordenados e desordenados de cilindros

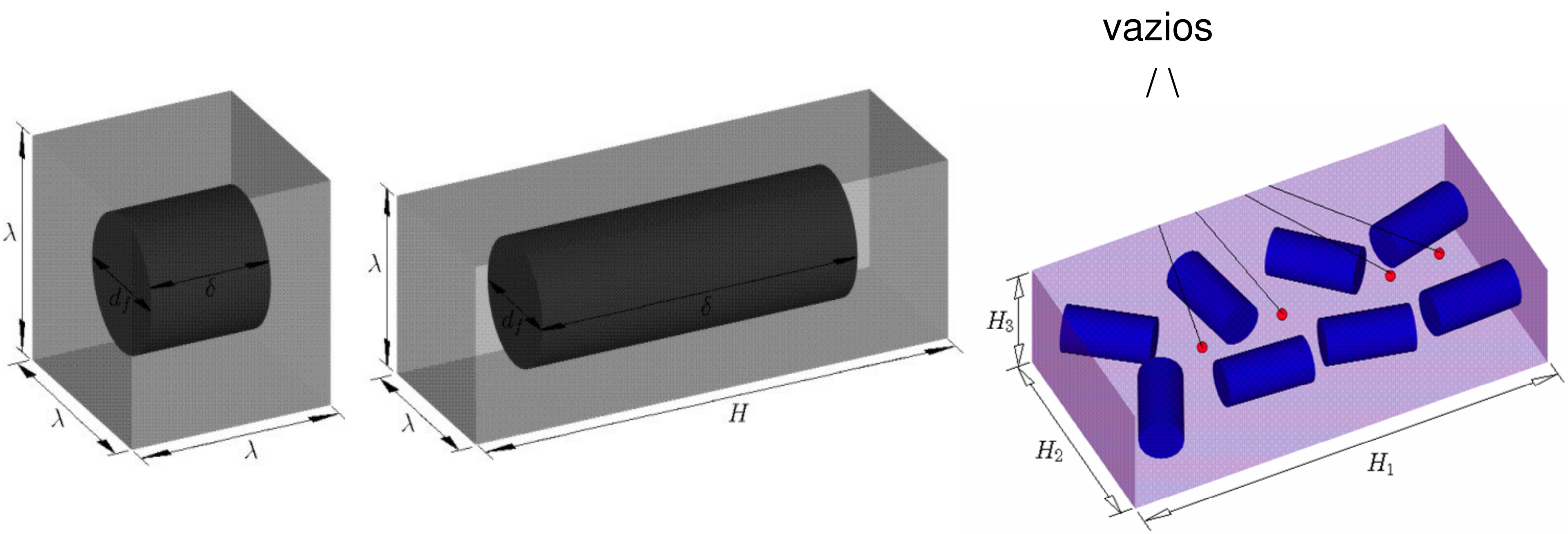

MÉTODOS NUMÉRICOS (cont.)

- GERAÇÃO DE MALHAS EM 3-D

  Procedimento baseado no gerador NETGEN (Schöberl, 2002)

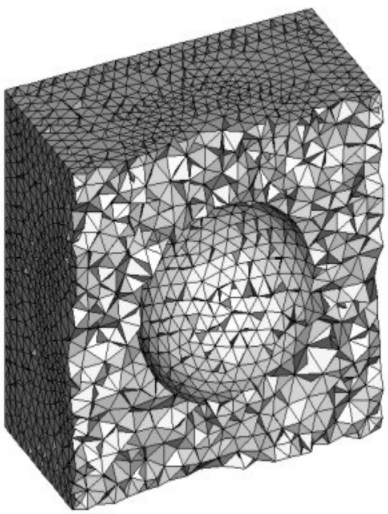

$c = 0{,}10$

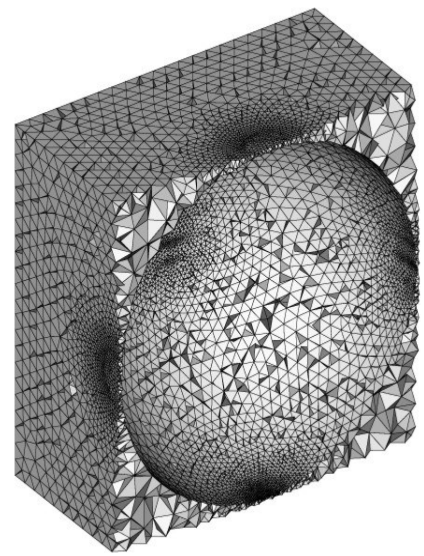

$c = 0{,}50$

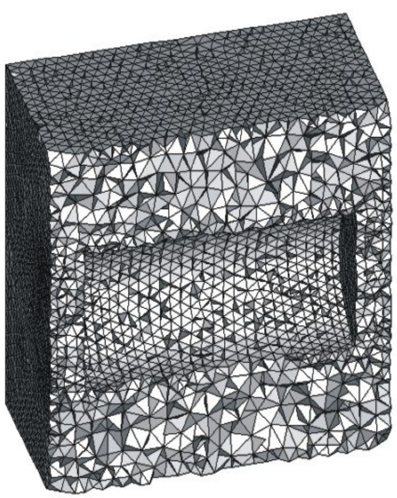

$c = 0{,}10$

$\rho = 2$

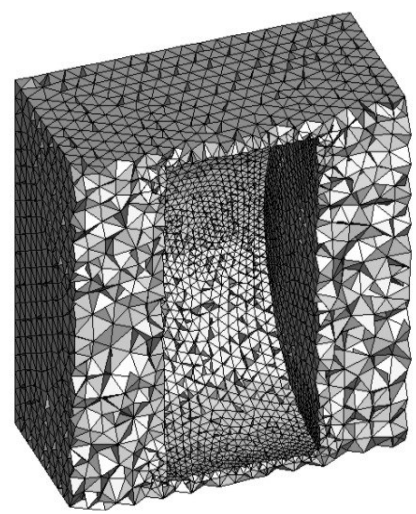

$c = 0{,}30$

$\rho = 0{,}5$

MÉTODOS NUMÉRICOS (cont.)

- GERAÇÃO DE MALHAS EM 3-D
  Procedimento baseado no gerador NETGEN (Schöberl, 2002)

$c = 0{,}75$

$\rho_p = \rho_f = 5$

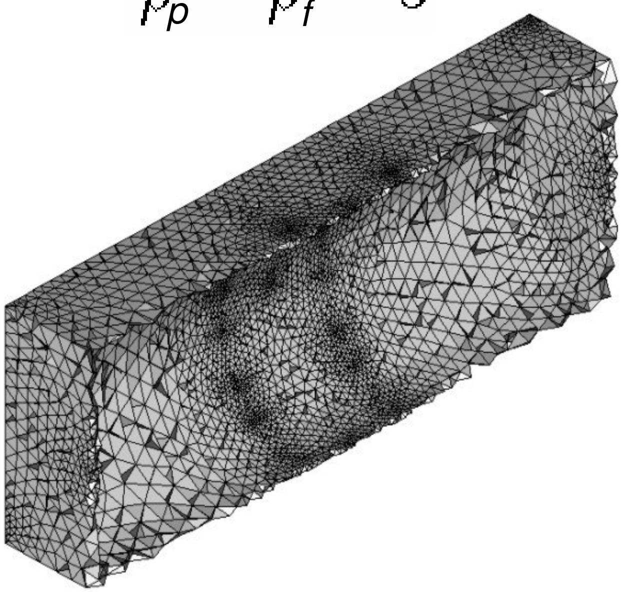

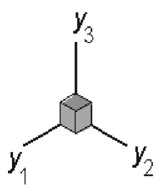

$c = 0.15$

$\rho_f = 2 \ \rho_p = 4$

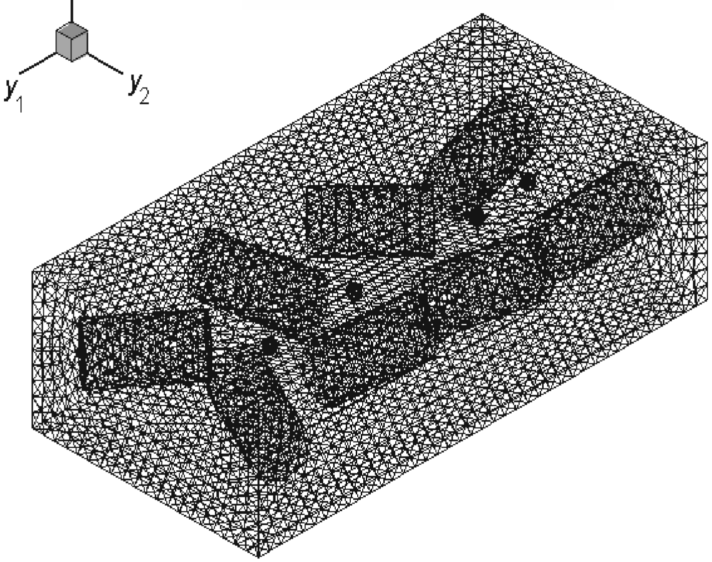

$c = 0.15$

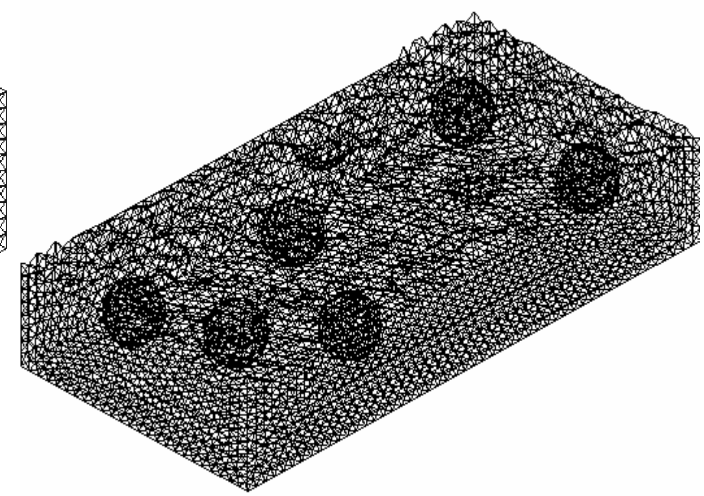

MÉTODOS NUMÉRICOS (cont.)

- DISCRETIZAÇÃO POR ELEMENTOS FINITOS
  - Isoparamétrica de primeira ordem
    - ✓ Solução e geometria interpoladas por polinômios de 1º grau
    - ✓ Implementação computacional mais simples
    - ✓ Integrais de volume e de superfície podem ser avaliadas analiticamente
    - ✓ Convergência quadrática da solução numérica
    - ✓ Resultados acurados para $k_{ij} > 100$ somente com refinamento excessivo da malha, onerando o tempo computacional
  - Isoparamétrica de segunda ordem
    - ✓ Solução e geometria interpoladas por polinômios de 2º grau
    - ✓ Implementação computacional mais sofisticada
    - ✓ Integrais de volume e de superfície tem que ser avaliadas numericamente
    - ✓ Convergência cúbica da solução numérica
    - ✓ Resultados acurados para $k_{ij} > 100$ sem a necessidade de um refinamento excessivo da malha

MÉTODOS NUMÉRICOS (cont.)

- DISCRETIZAÇÃO POR ELEMENTOS FINITOS

Problema da célula

$$a(v, \chi_p^{\mathrm{II}}) + b_\Gamma(v, \chi_p^{\mathrm{II}}) = \ell(v) \quad \forall v \in Y^{\mathrm{II}}(\Omega_{pc})$$

$$a(v, \chi_p^{\mathrm{II}}) = \int_{\Omega_{pc}} \zeta_{ij}(\mathbf{y}) \frac{\partial \chi_p^{\mathrm{II}}}{\partial y_j} \frac{\partial v}{\partial y_i} \, d\mathbf{y}$$

operador bilinear, simétrico e positivo-definido

$$\ell(v) = \int_{\Omega_{pc}} \zeta_{ip}(\mathbf{y}) \frac{\partial v}{\partial y_i} \, d\mathbf{y}$$

funcional linear relacionado à direção do gradiente de temperatura imposto externamente

$$b_\Gamma(v, \chi_p^{\mathrm{II}}) = \int_\Gamma \mathrm{Bi} \, [\chi_p^{\mathrm{II}}]_\Gamma \, [v]_\Gamma \, ds$$

operador bilinear e simétrico

MÉTODOS NUMÉRICOS (cont.)

- TRATAMENTO DAS INTEGRAIS DE VOLUME

Método de Galerkin (Reddy, 1993; Hughes, 1987)

$$\chi_p^e \equiv \chi_p^{II}|_{\Omega^e} = \sum_{a=1}^{10} \chi_{p,a}^e \psi_a^e$$

$$v^e \equiv v|_{\Omega^e} = \sum_{b=1}^{10} v_b^e \psi_b^e$$

$$\Rightarrow$$

$$a(v^e, \chi_p^e) \rightarrow k_{ab}^e$$

$$\ell(v^e) \rightarrow f_a^e$$

$$\mathbf{J}^e = \frac{\partial(y_1, y_2, y_3)}{\partial(\xi, \eta, \zeta)}$$

$$f_a^e = \int_{\Omega^e} \zeta_{ip}^e \frac{\partial \psi_a^e}{\partial y_i} \, d\mathbf{y} = \int_0^1 \int_0^{1-\xi} \int_0^{1-\xi-\eta} \zeta_{ip}^e \left(\frac{\partial \psi_a^e}{\partial \xi} \frac{\partial \xi}{\partial y_i} + \frac{\partial \psi_a^e}{\partial \eta} \frac{\partial \eta}{\partial y_i} + \frac{\partial \psi_a^e}{\partial \zeta} \frac{\partial \zeta}{\partial y_i} \right) \det \mathbf{J}^e \; d\zeta \, d\eta \, d\xi$$

$$\begin{aligned} k_{ab}^e &= \int_{\Omega^e} \zeta_{ij}^e \frac{\partial \psi_a^e}{\partial y_j} \frac{\partial \psi_b^e}{\partial y_i} \, d\mathbf{y} \\ &= \int_0^1 \int_0^{1-\xi} \int_0^{1-\xi-\eta} \zeta_{ij}^e \left(\frac{\partial \psi_a^e}{\partial \xi} \frac{\partial \xi}{\partial y_j} + \frac{\partial \psi_a^e}{\partial \eta} \frac{\partial \eta}{\partial y_j} + \frac{\partial \psi_a^e}{\partial \zeta} \frac{\partial \zeta}{\partial y_j} \right) \left(\frac{\partial \psi_b^e}{\partial \xi} \frac{\partial \xi}{\partial y_j} + \frac{\partial \psi_b^e}{\partial \eta} \frac{\partial \eta}{\partial y_j} + \frac{\partial \psi_b^e}{\partial \zeta} \frac{\partial \zeta}{\partial y_j} \right) \det \mathbf{J}^e \; d\zeta \, d\eta \, d\xi \end{aligned}$$

MÉTODOS NUMÉRICOS (cont.)

- TRATAMENTO DA INTEGRAL DE SUPERFÍCIE

  - Duplicação dos graus de liberdade associados aos nós globais situados sobre a interface Γ

  - Modificação da conectividade dos tetraedros que possuem pelo menos um nó sobre Γ

  - Cálculo dos saltos das funções (peso, teste) através das superfícies em Γ

  - Integração do produto dos saltos em Γ

  - Soma das integrais resultantes aos componentes apropriados da matriz de rigidez global

DUPLICAÇÃO DOS GRAUS DE LIBERDADE E MODIFICAÇÃO DA CONECTIVIDADE DOS TETRAEDROS

ANTES DA DUPLICAÇÃO

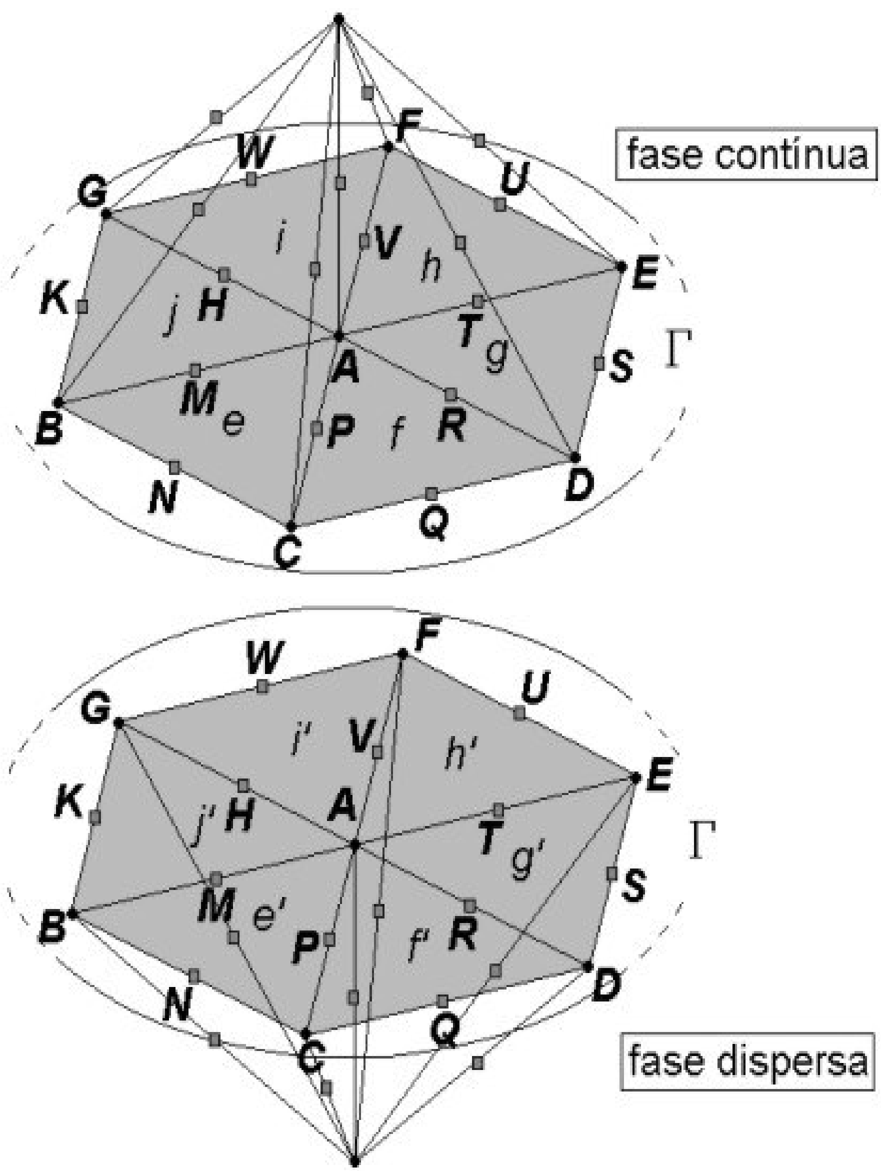

APÓS A DUPLICAÇÃO

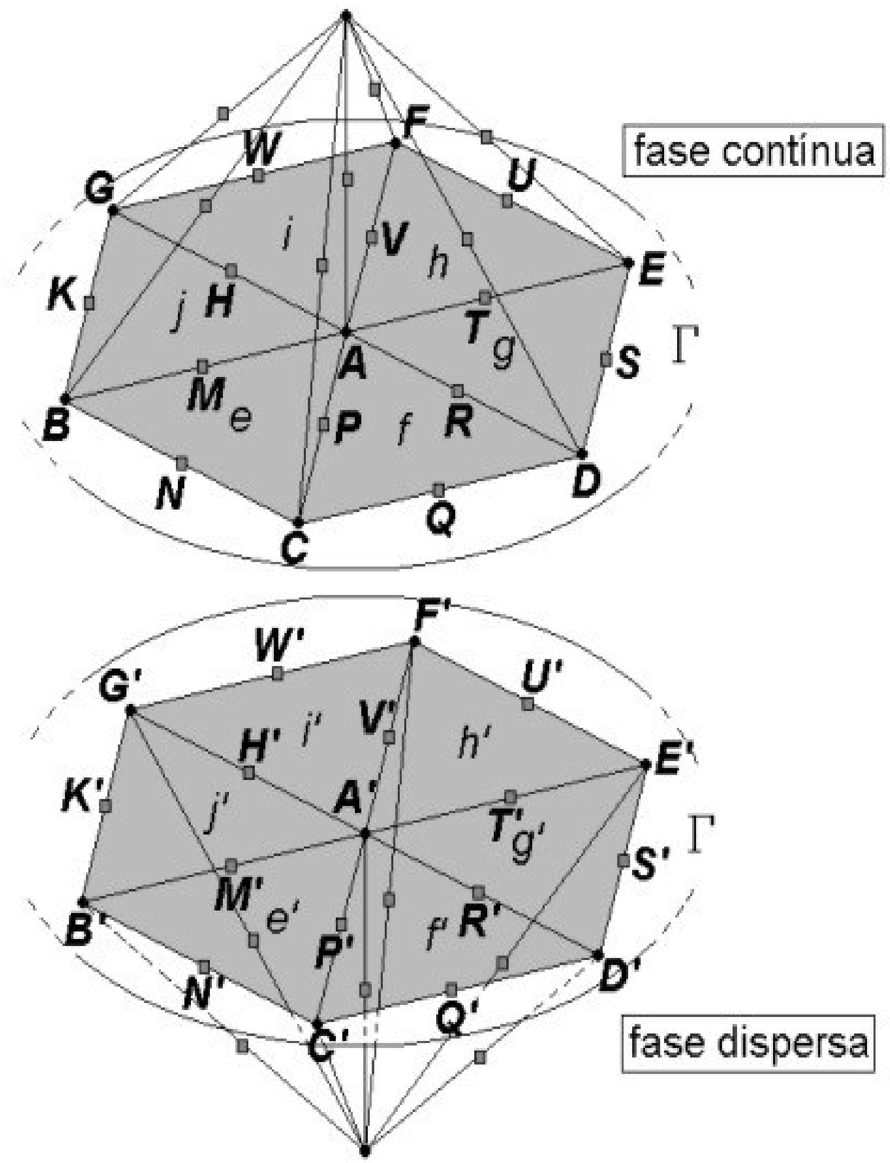

MÉTODOS NUMÉRICOS (cont.)

- Contribuições associadas ao nó do vértice *A*

  - Função peso restrita ao nó *A*

$$v_A\big|_{e,\Gamma} = \phi_A^c\big|_{e,\Gamma}$$

  - Salto da função peso através de $\Gamma_{ee'}$

$$[v_A]_{\Gamma_{ee'}} = v_A\big|_{e,\Gamma} - \overbrace{v_A\big|_{e',\Gamma}}^{0} = v_A\big|_{e,\Gamma} = \phi_A^c\big|_{e,\Gamma}$$

  - Salto da temperatura através de $\Gamma_{ee'}$ $\quad \left[\chi_{p,h}^{\mathrm{II}}\right]_{\Gamma_{ee'}} = \chi_{p,h}^{\mathrm{II},c}\big|_{e,\Gamma} - \chi_{p,h}^{\mathrm{II},d}\big|_{e',\Gamma}$

$$\left[\chi_{p,h}^{\mathrm{II}}\right]_{\Gamma_{ee'}} = \chi_A\,\phi_A^c\big|_{e,\Gamma} + \chi_B\,\phi_B^c\big|_{e,\Gamma} + \chi_C\,\phi_C^c\big|_{e,\Gamma} + \chi_M\,\phi_M^c\big|_{e,\Gamma} + \chi_N\,\phi_N^c\big|_{e,\Gamma} + \chi_P\,\phi_P^c\big|_{e,\Gamma} -$$

$$\chi_{A'}\,\phi_{A'}^d\big|_{e',\Gamma} - \chi_{B'}\,\phi_{B'}^d\big|_{e',\Gamma} - \chi_{C'}\,\phi_{C'}^d\big|_{e',\Gamma} - \chi_{M'}\,\phi_{M'}^d\big|_{e',\Gamma} - \chi_{N'}\,\phi_{N'}^d\big|_{e',\Gamma} - \chi_{P'}\,\phi_{P'}^d\big|_{e',\Gamma}$$

MÉTODOS NUMÉRICOS (cont.)

- Contribuições associadas ao nó do vértice *A*

somar ao componente K_{AA}

$$\int_{\Gamma_{ee'}} \mathrm{Bi}\ [v_A]_{\Gamma_{ee'}}\ [\chi_{p,h}^{\mathrm{II}}]_{\Gamma_{ee'}} d\mathbf{s} = \mathrm{Bi} \Bigg(\chi_A \boxed{\int_{\Gamma_{ee'}} \phi_A^c|_{e,\Gamma}\ \phi_A^c|_{e,\Gamma}\ d\mathbf{s}} + \chi_B \int_{\Gamma_{ee'}} \phi_A^c|_{e,\Gamma}\ \phi_B^c|_{e,\Gamma}\ d\mathbf{s} +$$
$$\chi_C \int_{\Gamma_{ee'}} \phi_A^c|_{e,\Gamma}\ \phi_C^c|_{e,\Gamma}\ d\mathbf{s} + \chi_M \int_{\Gamma_{ee'}} \phi_A^c|_{e,\Gamma}\ \phi_M^c|_{e,\Gamma}\ d\mathbf{s} + \chi_N \int_{\Gamma_{ee'}} \phi_A^c|_{e,\Gamma}\ \phi_N^c|_{e,\Gamma}\ d\mathbf{s} +$$
$$\chi_P \int_{\Gamma_{ee'}} \phi_A^c|_{e,\Gamma}\ \phi_P^c|_{e,\Gamma}\ d\mathbf{s} - \chi_{A'} \int_{\Gamma_{ee'}} \phi_A^c|_{e,\Gamma}\ \phi_{A'}^d|_{e',\Gamma}\ d\mathbf{s} - \chi_{B'} \int_{\Gamma_{ee'}} \phi_A^c|_{e,\Gamma}\ \phi_{B'}^d|_{e',\Gamma}\ d\mathbf{s} -$$
$$\chi_{C'} \int_{\Gamma_{ee'}} \phi_A^c|_{e,\Gamma}\ \phi_{C'}^d|_{e',\Gamma}\ d\mathbf{s} - \chi_{M'} \int_{\Gamma_{ee'}} \phi_A^c|_{e,\Gamma}\ \phi_{M'}^d|_{e',\Gamma}\ d\mathbf{s} - \chi_{N'} \int_{\Gamma_{ee'}} \phi_A^c|_{e,\Gamma}\ \phi_{N'}^d|_{e',\Gamma}\ d\mathbf{s} -$$
$$\chi_{P'} \int_{\Gamma_{ee'}} \phi_A^c|_{e,\Gamma}\ \phi_{P'}^d|_{e',\Gamma}\ d\mathbf{s} \Bigg)$$

MÉTODOS NUMÉRICOS (cont.)

- Algoritmo

Para cada nó situado sobre Γ

- Identificação dos nós vizinhos (de vértice e medianos)
- Identificação de seu duplicado e dos duplicados de seus vizinhos
- Definição da função peso restrita ao nó e aos tetraedros que o compartilham em Γ
- Cálculo dos saltos da função peso e da temperatura através das superfícies dos tetraedros que compartilham o nó em Γ
- Avaliação das integrais resultantes
- Soma das integrais resultantes aos componentes apropriados da matriz de rigidez global

SISTEMA DISCRETO DE EQUAÇÕES $\mathcal{K}^* \chi_{p,h}^{\mathrm{II}} = \mathcal{F}^*$

MATRIZ DE RIGIDEZ E VETOR DE CARGA GLOBAIS MONTADOS A PARTIR DAS MATRIZES E VETORES ELEMENTARES, IMPONDO-SE AS CONDIÇÕES DE CONTORNO DE PERIODICIDADE NAS SUPERFÍCIES DE Ω_{pc}

MÉTODOS NUMÉRICOS (cont.)

- Método iterativo (mínimos resíduos; Paige & Saunders, 1975)

  - Apropriado para sistemas lineares de equações em que a matriz dos coeficientes é simétrica mas não necessariamente positiva-definida

  - Critério de parada: baseado na norma L_2 do vetor resíduo e em uma tolerância especificada pelo 'usuário' (σ)

$$\mathbf{A}\,\mathbf{u} = \mathbf{b}$$

$$\mathbf{r} \equiv \mathbf{b} - \mathbf{A}\,\mathbf{u}^{*} \qquad \mathbf{r}_0 \equiv \mathbf{b} - \mathbf{A}\,\mathbf{u}^{*(0)}$$

$$||\mathbf{r}||_{L_2} = \left(\mathbf{r}^T\,\mathbf{r}\right)^{1/2} \qquad ||\mathbf{r}_0||_{L_2} = \left(\mathbf{r}_0^T\,\mathbf{r}_0\right)^{1/2}$$

$$\frac{||\mathbf{r}||_{L_2}}{||\mathbf{r}_0||_{L_2}} < \sigma^2$$

FIM!!

MUITO OBRIGADO!!

RESULTADOS

RESULTADOS

- Esforço 2-D: menor do que o esforço 3-D e (ainda) vale a pena no caso de arranjos randômicos
- Arranjo cúbico simples de esferas com resistência térmica interfacial uniforme (e, também, com contato térmico perfeito)
- Arranjo desordenado de esferas com resistência térmica interfacial uniforme e poros na matriz (cálculos ilustrativos)
- Arranjo paralelepipedal de cilindros com resistência térmica interfacial uniforme
- Tentativa de comparação com dados experimentais

DETERMINAÇÃO DA CONDUTIVIDADE TÉRMICA EFETIVA DE COMPÓSITOS FIBROSOS UNIDIRECIONAIS RANDÔMICOS

Leandro Bastos Machado

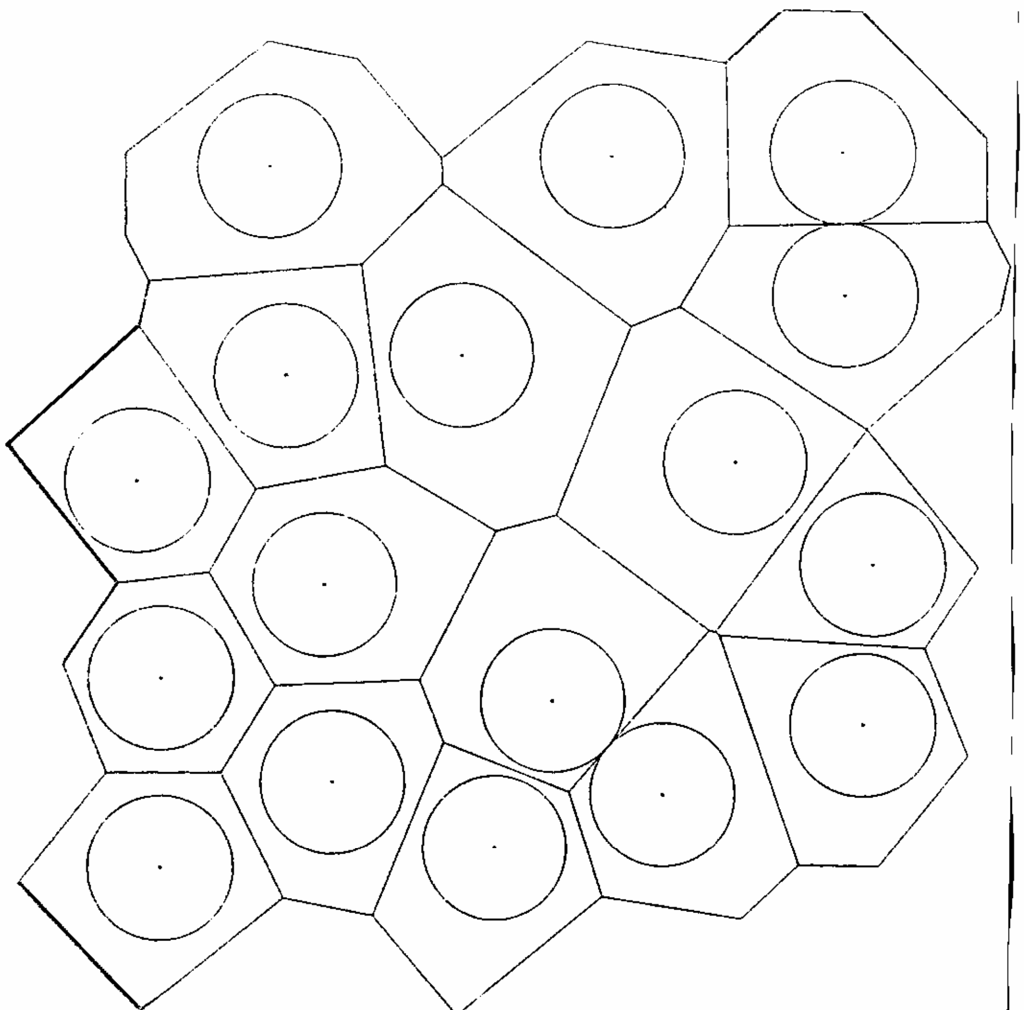

Figura 6.8: A célula de Voronoi com 17 fibras e $c = 0,375$.

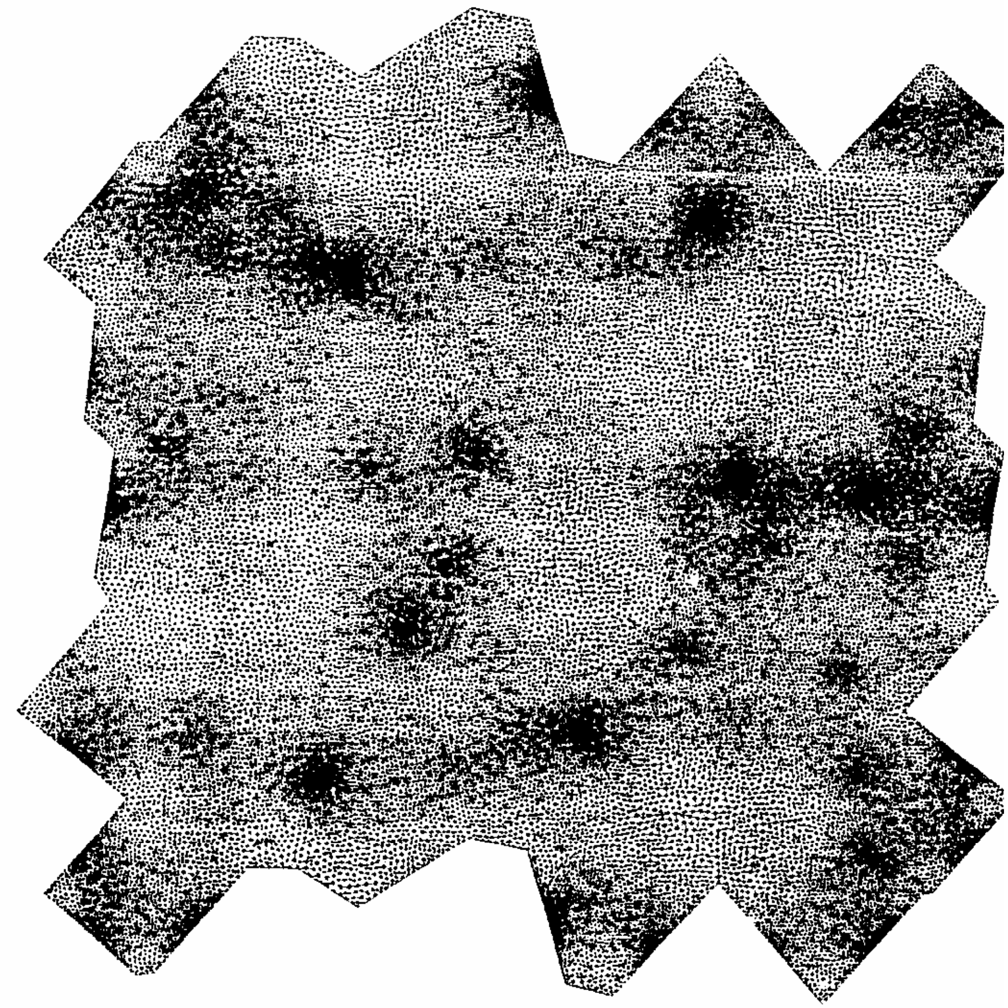

Figura 6.10: Malha para as realizações com 32 fibras e $c = 0,5$.

XV Congresso Brasileiro de Engenharia Mecânica
15th Brazilian Congress of Mechanical Engineering
22 - 26 de Novembro de 1999 / November 22 - 26, 1999 Águas de Lindóia, São Paulo

BOUNDS FOR THE EFFECTIVE CONDUCTIVITY OF UNIDIRECTIONAL COMPOSITES BASED ON ISOTROPIC MICROSCALE MODELS

eandro B. Machado
anuel E. Cruz
deral University of Rio de Janeiro, EE/COPPE, Department of Mechanical Engineering
. P. 68503 — 21945–970 — Rio de Janeiro, RJ, Brazil
mail: manuel@serv.com.ufrj.br

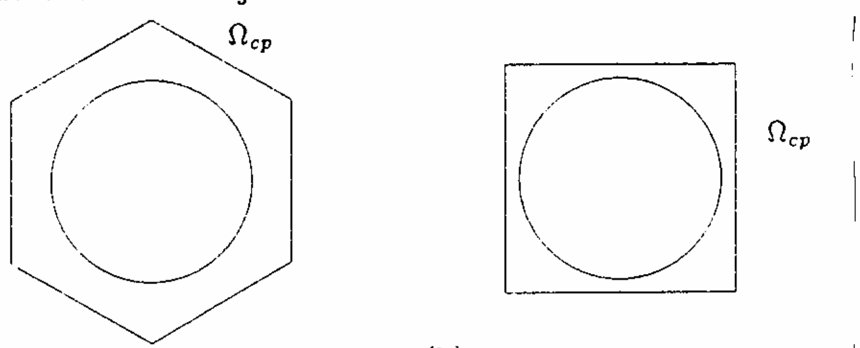

ura 6.1: Células periódicas dos arranjos ordenados triangular (a) e quadrado (b).

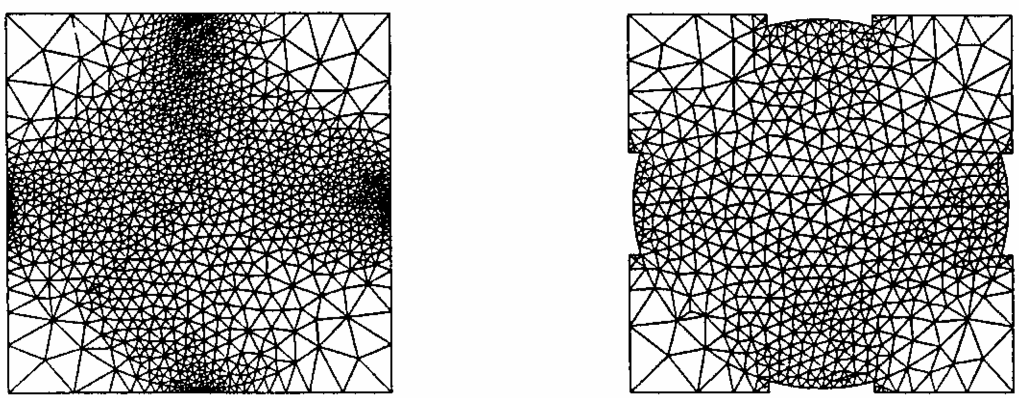

gure 2: Illustrative finite element meshes for the square array, $c = 0.75$: mesh on the ft is for Ω_{pc} ($\mathcal{N} = 0$), and mesh on the right is for both $\mathcal{L}$ and $\mathcal{U}$ ($\mathcal{N} = 2$).

c	α							
	2			10			50	
	β	k_e	$k_{e,h}$	β	k_e	$k_{e,h}$	β	k_e
		1.6767	1.677		4.9443	4.946		9.5355
		$k_{LB,h}$	$k_{UB,h}$		$k_{LB,h}$	$k_{UB,h}$		$k_{LB,h}$
0.75	0.06	1.620	1.686	0.06	4.240	5.833	0.06	6.793
		$\overline{k}_{e,h}$	$\overline{E}_r$		$\overline{k}_{e,h}$	$\overline{E}_r$		$\overline{k}_{e,h}$
		1.65	2.0%		5.0	16%		15
		$k_{LB,h}$	$k_{UB,h}$		$k_{LB,h}$	$k_{UB,h}$		$k_{LB,h}$
	0.04	1.647	1.683	0.04	4.524	5.653	0.04	7.714
		$\overline{k}_{e,h}$	$\overline{E}_r$		$\overline{k}_{e,h}$	$\overline{E}_r$		$\overline{k}_{e,h}$
		1.67	1.1%		5.1	11%		15
	β	k_e	$k_{e,h}$	β	k_e	$k_{e,h}$	β	k_e
		1.7154	1.715		5.8037	5.805		16.310
		$k_{LB,h}$	$k_{UB,h}$		$k_{LB,h}$	$k_{UB,h}$		$k_{LB,h}$
0.78	0.06	1.671	1.719	0.06	4.983	6.126	0.06	9.575
		$\overline{k}_{e,h}$	$\overline{E}_r$		$\overline{k}_{e,h}$	$\overline{E}_r$		$\overline{k}_{e,h}$
		1.70	1.4%		5.6	10%		17
		$k_{LB,h}$	$k_{UB,h}$		$k_{LB,h}$	$k_{UB,h}$		$k_{LB,h}$
	0.04	1.695	1.717	0.04	5.369	6.004	0.04	11.76
		$\overline{k}_{e,h}$	$\overline{E}_r$		$\overline{k}_{e,h}$	$\overline{E}_r$		$\overline{k}_{e,h}$
		1.71	0.64%		5.7	5.6%		17
	β	k_e	$k_{e,h}$	β	k_e	$k_{e,h}$	β	k_e
		1.7220	—		6.004	—		20.5
		$k_{LB,h}$	$k_{UB,h}$		$k_{LB,h}$	$k_{UB,h}$		$k_{LB,h}$
0.785	0.06	1.680	1.724	0.06	5.16	6.19	0.06	10.5
		$\overline{k}_{e,h}$	$\overline{E}_r$		$\overline{k}_{e,h}$	$\overline{E}_r$		$\overline{k}_{e,h}$
		1.70	1.3%		5.7	9.0%		18
		$k_{LB,h}$	$k_{UB,h}$		$k_{LB,h}$	$k_{UB,h}$		$k_{LB,h}$
	0.04	1.704	1.723	0.04	5.59	6.08	0.04	13.5
		$\overline{k}_{e,h}$	$\overline{E}_r$		$\overline{k}_{e,h}$	$\overline{E}_r$		$\overline{k}_{e,h}$
		1.713	0.55%		5.8	4.2%		18
	β	k_e	$k_{e,h}$	β	k_e	$k_{e,h}$	β	k_e
		—	—		—	—		—
		$k_{LB,h}$	$k_{UB,h}$		$k_{LB,h}$	$k_{UB,h}$		$k_{LB,h}$
$\pi/4$	0.06	1.681	1.725	0.06	5.18	6.19	0.06	10.6
		$\overline{k}_{e,h}$	$\overline{E}_r$		$\overline{k}_{e,h}$	$\overline{E}_r$		$\overline{k}_{e,h}$
		1.70	1.3%		5.7	8.9%		18
		$k_{LB,h}$	$k_{UB,h}$		$k_{LB,h}$	$k_{UB,h}$		$k_{LB,h}$
	0.04	1.705	1.723	0.04	5.61	6.09	0.04	13.7
		$\overline{k}_{e,h}$	$\overline{E}_r$		$\overline{k}_{e,h}$	$\overline{E}_r$		$\overline{k}_{e,h}$
		1.714	0.53%		5.9	4.1%		18

Table 1: Effective conductivity results for the square array

Parameters: $c \in \{0.75, 0.78, 0.785, \pi/4\}$, $\alpha \in \{2, 10, 50\}$, $\beta \in \{0.04, 0.06\}$.

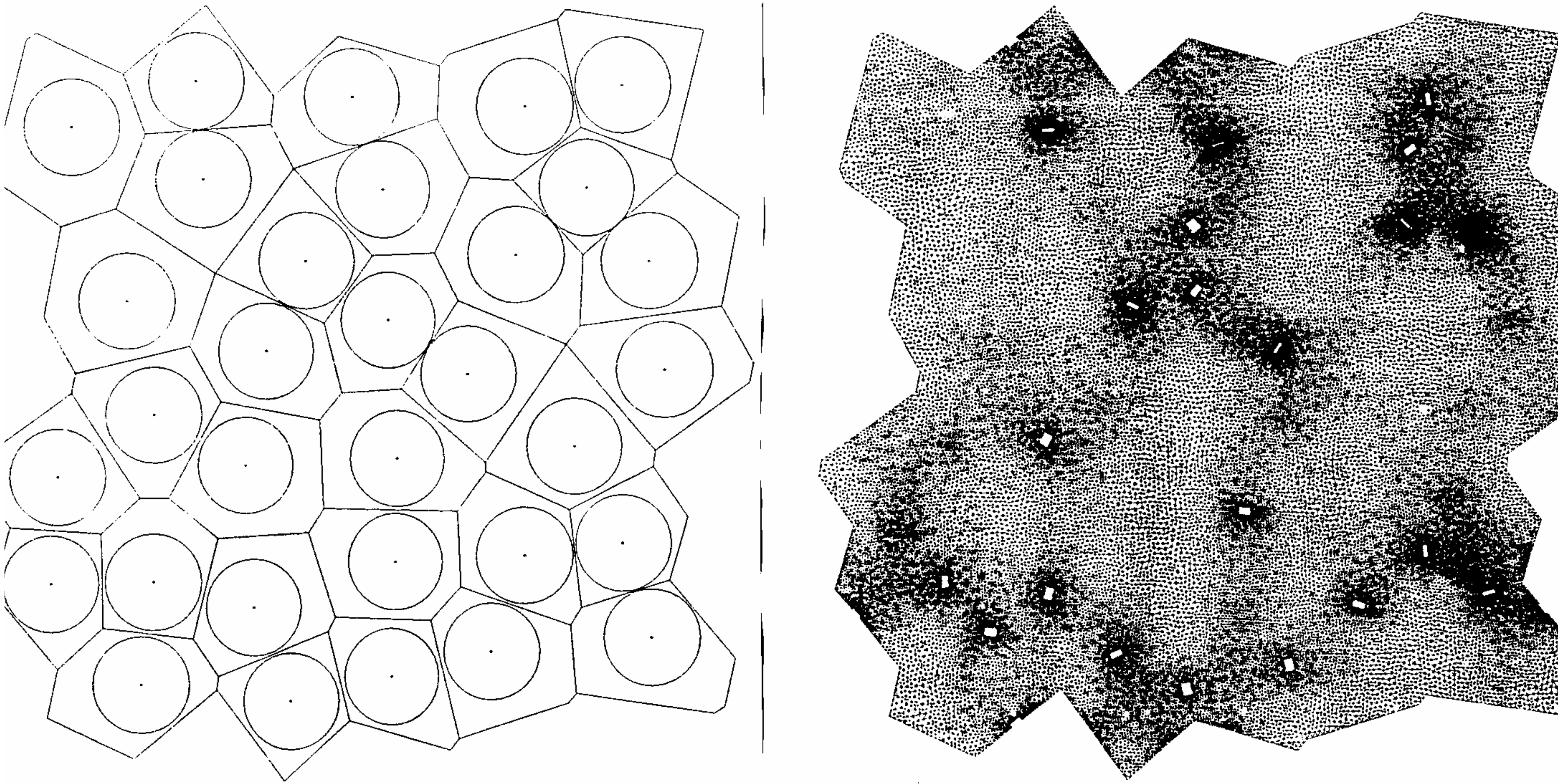

ura 6.14: Célula de Voronoi com 32 fibras e $c = 0,5$, onde a malha só pode ser
ada com a eliminação de regiões de estreito.

bela 6.10: Resultados obtidos para as realizações com *32 fibras*, $c = 0,5$ e $\alpha \in$ 10, 50}, onde a geração de malha é *possível*: numéricos, $k_{e,h}$, limites isotrópicos, $_{h}$ e $k_{\mathrm{SI},h}$, limites anisotrópicos, $k_{\mathrm{IA},h}$ e $k_{\mathrm{SA},h}$, estimativas para a condutividade, $\overline{k}_{\mathrm{I}}$ $_{\mathrm{A}}$, e erros relativos, $\overline{E}_{r,\mathrm{I}}$ e $\overline{E}_{r,\mathrm{A}}$. Parâmetros das regiões de estreito: $\beta = 0,06$ e $= 0,1$.

$\alpha = 2$								
$k_{e,h}$	$k_{\mathrm{II},h}$	$k_{\mathrm{SI},h}$	$\overline{k}_{\mathrm{I}}$	$\overline{E}_{r,\mathrm{I}}$	$k_{\mathrm{IA},h}$	$k_{\mathrm{SA},h}$	$\overline{k}_{\mathrm{A}}$	$\overline{E}$
1,410	1,397	1,413	1,4	5,5%	1,398	1,412	1,4	5,
$\alpha = 10$								
$k_{e,h}$	$k_{\mathrm{II},h}$	$k_{\mathrm{SI},h}$	$\overline{k}_{\mathrm{I}}$	$\overline{E}_{r,\mathrm{I}}$	$k_{\mathrm{IA},h}$	$k_{\mathrm{SA},h}$	$\overline{k}_{\mathrm{A}}$	$\overline{E}$
2,636	2,545	2,768	2,7	4,2%	2,545	2,758	2,7	4,
$\alpha = 50$								
$k_{e,h}$	$k_{\mathrm{II},h}$	$k_{\mathrm{SI},h}$	$\overline{k}_{\mathrm{I}}$	$\overline{E}_{r,\mathrm{I}}$	$k_{\mathrm{IA},h}$	$k_{\mathrm{SA},h}$	$\overline{k}_{\mathrm{A}}$	$\overline{E}$
3,454	3,239	4,134	3,7	12%	3,239	4,067	3,7	11

Extensão para 3 dimensões

Arranjo cúbico

ABSTRACT SUBMISSION

Authors should submit two copies of an abstract of approximately 500 words. Authors and co-authors are requested to provide their complete addresses, phone and fax numbers, and e-mail addresses.

The abstracts should be sent to:

Prof. R. M. Cotta/CHMT
Laboratory of Transmission and Technology of Heat LTTC
PEM/COPPE-DEM/EE
Universidade Federal do Rio de Janeiro
Cx Postal 68503, Rio de Janeiro 21945-970, Brazil

Phone: 55-21-5608832 Ext.412
Fax: 55-21-2906626
E-mail: chmt2001@lttc.coppe.ufrj.br
(for electronic submission)
Home page: www.lttc.com.ufrj.br

CALL FOR PAPERS

October 30th, 2000	**Due date of abstract**
December 30th, 2000	**Notification of abstract acceptance**
March 30th, 2001	**Due date of full paper**
May 30th, 2001	**Notification of paper acceptance**

Note: All accepted papers of pre-registered participants will appear in the proceedings of the conference. Selected papers will be recommended for publication in the Hybrid Methods in Engineering Journal, edited by Begell House, Inc.

22 - 26 October, 2001
Rio de Janeiro, Brazil

2nd International Conference on Computational Heat and Mass Transfer

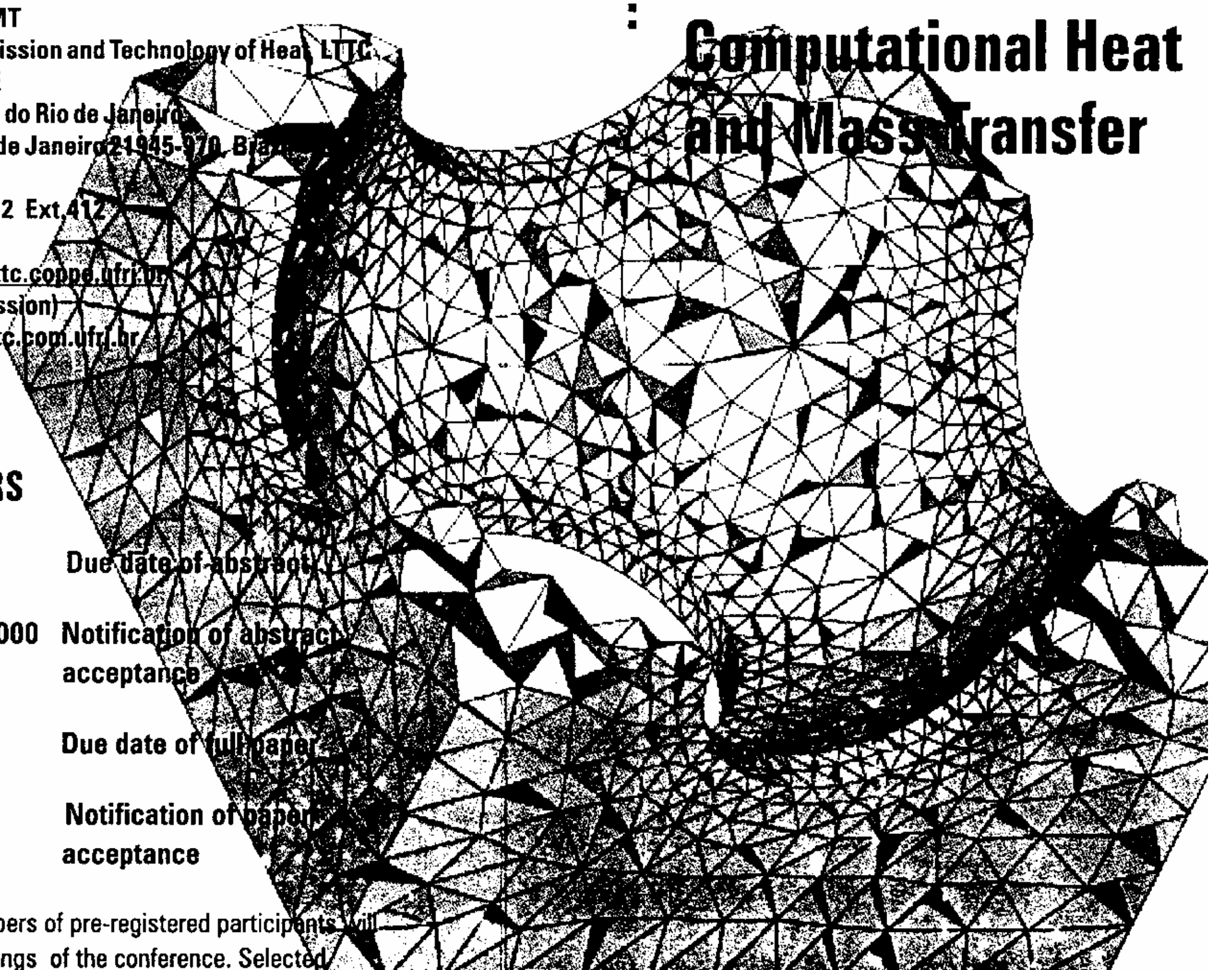

Promoted by
Universidade Federal do Rio de Janeiro
COPPE/EE/UFRJ, Brazil

ARRANJO CÚBICO SIMPLES DE ESFERAS

Validação com resultados semi-analíticos de Cheng & Torquato (1997)

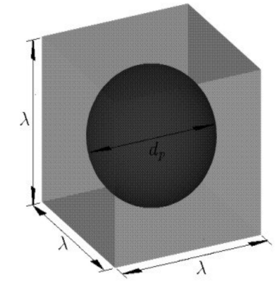

$$R_c = \kappa - 1$$

resistência térmica de contato crítica

c	$\alpha = 10,\ R_c = 9$				$\alpha = 10000,\ R_c = 9999$			
	$R = 5$		$R = 30$		$R = 5000$		$R = 20000$	
	κ_e^h	κ_e^{CT}	κ_e^h	κ_e^{CT}	κ_e^h	κ_e^{CT}	κ_e^h	κ_e^{CT}
0,05	1,0275	1,0275	0,9569	0,9569	1,0379	1,0380	0,9703	0,9703
0,10	1,0556	1,0556	0,9150	0,9150	1,0768	1,0769	0,9412	0,9412
0,15	1,0841	1,0841	0,8742	0,8742	1,1168	1,1168	0,9126	0,9126
0,20	1,1131	1,1132	0,8348	0,8348	1,1577	1,1578	0,8845	0,8845
0,25	1,1428	1,1428	0,7957	0,7957	1,1997	1,1998	0,8569	0,8569
0,30	1,1728	1,1729	0,7577	0,7577	1,2428	1,2429	0,8299	0,8298
0,35	1,2036	1,2036	0,7203	0,7203	1,2870	1,2870	0,8030	0,8029
0,40	1,2346	1,2347	0,6834	0,6833	1,3321	1,3322	0,7764	0,7763
0,45	1,2663	1,2663	0,6465	0,6464	1,3783	1,3783	0,7499	0,7498
0,50	1,2983	1,2983	0,6092	0,6091	1,4255	1,4254	0,7234	0,7232
0,51	1,3047	1,3047	0,6016	0,6015	1,4349	1,4349	0,7180	0,7178

ARRANJO CÚBICO SIMPLES DE ESFERAS

Comportamentos distintos para a condutividade térmica efetiva em função da magnitude da resistência térmica interfacial

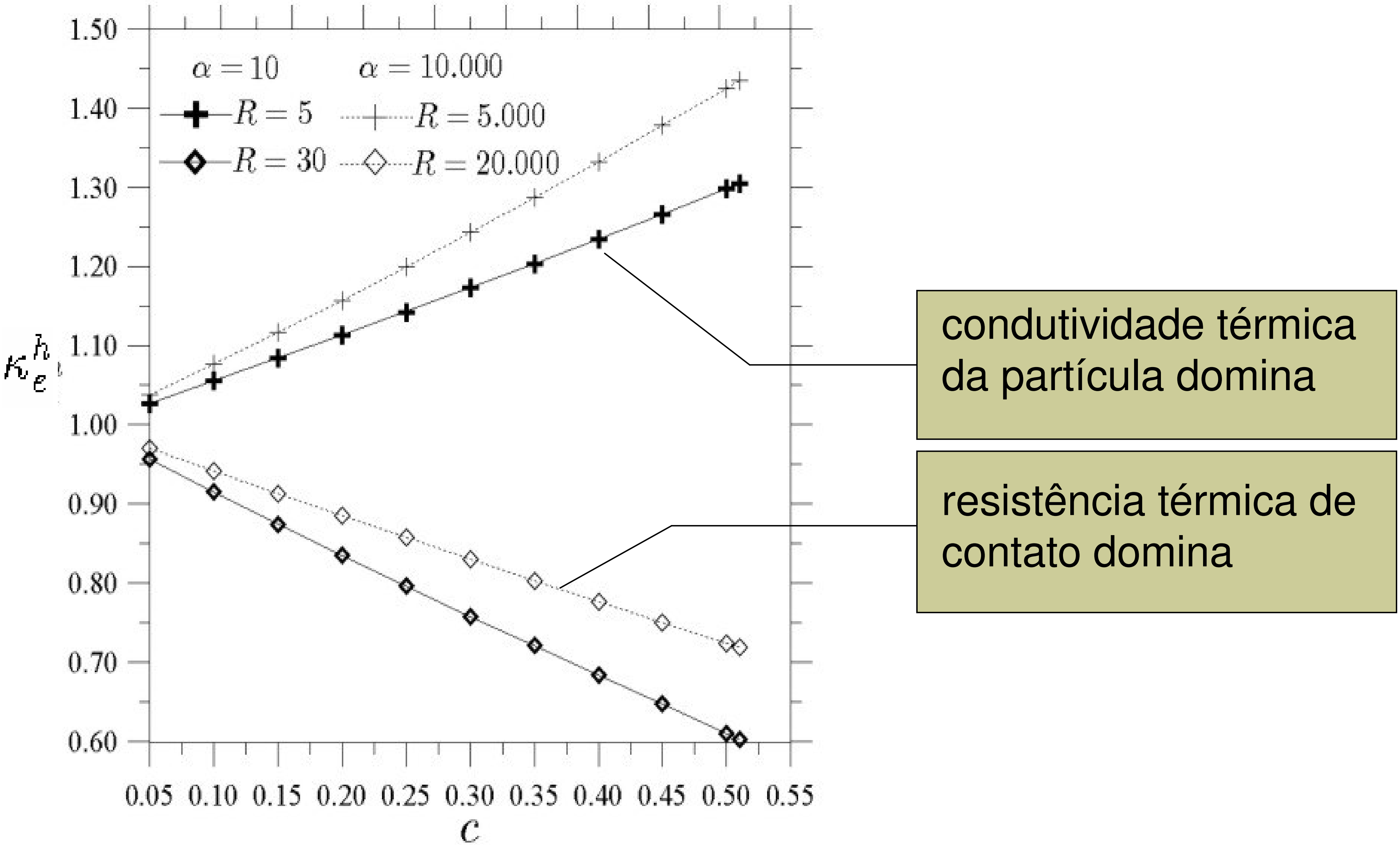

ARRANJO DESORDENADO DE ESFERAS COM RESISTÊNCIA TÉRMICA INTERFACIAL UNIFORME E POROS NO INTERIOR DA MATRIZ (CÁLCULOS ILUSTRATIVOS, ACURADOS: novidade!)

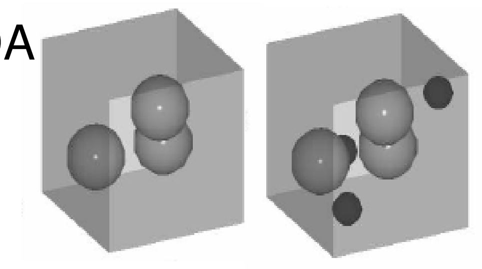

Values of $k_e^{\mathrm{N}}(\mathcal{C})$ for $c = 0.15$

$\alpha = 10, \quad R_c = 9$

	Without voids		With 0.56% voids	
$\mathcal{C}$	$R = 5$	$R = 30$	$R = 5$	$R = 30$
1	1.0286	0.8509	1.0256	0.8469
2	1.0284	0.8466	1.0250	0.8440
3	1.0288	0.8571	1.0254	0.8543
4	1.0286	0.8518	1.0253	0.8490
5	1.0287	0.8557	1.0257	0.8525
6	1.0287	0.8535	1.0255	0.8502
7	1.0284	0.8462	1.0252	0.8424
8	1.0287	0.8548	1.0256	0.8502
9	1.0282	0.8409	1.0251	0.8371
10	1.0280	0.8337	1.0248	0.8305
$\overline{k_e^{\mathrm{N}}}$	1.0285	0.849	1.0253	0.846
$S_{k_e^{\mathrm{N}}}$	0.0003	0.007	0.0003	0.007
k_e^{B}	1.0308	0.851	—	—

Values of $k_e^{\mathrm{N}}(\mathcal{C})$ for $c = 0.15$

$\alpha = 10000, \quad R_c = 9999$

	Without voids		With 0.56% voids	
$\mathcal{C}$	$R = 5000$	$R = 20000$	$R = 5000$	$R = 20000$
1	1.0497	0.8789	1.0469	0.8751
2	1.0492	0.8761	1.0457	0.8733
3	1.0505	0.8831	1.0470	0.8802
4	1.0498	0.8795	1.0465	0.8766
5	1.0503	0.8821	1.0472	0.8790
6	1.0500	0.8807	1.0469	0.8774
7	1.0492	0.8758	1.0460	0.8721
8	1.0502	0.8816	1.0473	0.8772
9	1.0487	0.8724	1.0457	0.8688
10	1.0480	0.8678	1.0448	0.8646
$\overline{k_e^{\mathrm{N}}}$	1.0496	0.878	1.0464	0.874
$S_{k_e^{\mathrm{N}}}$	0.0008	0.005	0.0008	0.005
k_e^{B}	1.0522	0.880	—	—

ARRANJO PARALELEPIPEDAL DE CILINDROS

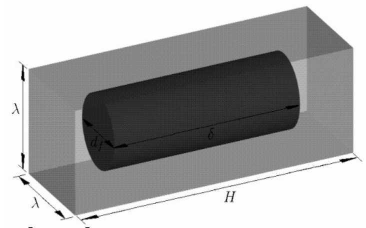

Validação com os resultados obtidos a partir da regra de misturas e a partir da expressão de Hasselman & Johnson (1987) para compósitos fibrosos unidirecionais com pequeno *c*

c = 0,10, ρ_p = 5 e α = 100						
ρ_f	Bi = 10^{-6}		Bi = 10^{-1}		Bi = 10^{2}	
	$\kappa_{11}^{e,h}$	$\kappa_{22}^{e,h}$	$\kappa_{11}^{e,h}$	$\kappa_{22}^{e,h}$	$\kappa_{11}^{e,h}$	$\kappa_{22}^{e,h}$
6	0,8852	0,8335	0,9619	0,8401	1,9352	1,2283
8	0,8902	0,8286	0,9991	0,8349	2,3972	1,2160
12	0,8956	0,8226	1,0839	0,8285	4,1371	1,2023
13,5	0,8981	0,8204	1,1214	0,8262	5,8827	1,1964
$\rho_{f,\,max}$ = 14	10,900	0,8182	10,900	0,8240	10,900	1,1920
	$\kappa_{e,L}^{RM}$	$\kappa_{e,T}^{H}$	$\kappa_{e,L}^{RM}$	$\kappa_{e,T}^{H}$	$\kappa_{e,L}^{RM}$	$\kappa_{e,T}^{H}$
	10,900	0,8182	10,900	0,8240	10,900	1,1920

ARRANJO PARALELEPIPEDAL DE CILINDROS

EXEMPLOS DE RESULTADOS NOVOS

ARRANJO PARALELEPIPEDAL $\rho_p = \rho_f = 20$								
c	$\alpha = 10$				$\alpha = 1000$			
	Bi = 10^{-6}		Bi = 10^4		Bi = 10^{-6}		Bi = 10^4	
	$\kappa_{11}^{e,h}$	$\kappa_{22}^{e,h}$	$\kappa_{11}^{e,h}$	$\kappa_{22}^{e,h}$	$\kappa_{11}^{e,h}$	$\kappa_{22}^{e,h}$	$\kappa_{11}^{e,h}$	$\kappa_{22}^{e,h}$
0,10	0,8872	0,8356	1,4647	1,2005	0,8872	0,8356	1,9586	1,2586
0,20	0,7710	0,6971	1,8674	1,4490	0,7710	0,6971	2,6674	1,5990
0,30	0,6584	0,5743	2,3184	1,7568	0,6584	0,5743	3,5628	2,0540
0,40	0,5520	0,4613	2,8671	2,1432	0,5520	0,4613	4,8528	2,6847
0,50	0,4530	0,3541	3,5772	2,6441	0,453	0,354	6,977	3,627
0,60	0,3619	0,2492	4,5568	3,3292	0,362	0,249	11,27	5,244
0,70	0,2785	0,1406	6,0220	4,3667	0,278	0,141	25,03	9,094

COMPARAÇÃO COM DADOS EXPERIMENTAIS (tentativa)

- Trabalho experimental de Mirmira (1999)
  - Medidas das condutividades térmicas efetivas longitudinal e transversal de compósitos de fibras curtas em função da temperatura
  - Características dos compósitos
    - ✓ Matriz: éster cianato
    - ✓ Fase dispersa: fibras de carbono (DKE X, DKA X, K22XX)
    - ✓ Fração volumétrica das fibras nos compósitos fabricados: 55%, 65% e 75%
    - ✓ Razão de aspecto das fibras: 20
    - ✓ Fração volumétrica de poros: 4% (estimativa)
    - ✓ Condutância térmica interfacial estimada: 10^5 W/m^2 K
    - ✓ Fibras distribuídas em planos paralelos e orientadas de forma aleatória
- Resultados numéricos: aplicação da metodologia desenvolvida ao arranjo paralelepipedal de cilindros
- Resultados analíticos: expressões para as condutividades efetivas obtidas por outros autores para arranjos de fibras cilíndricas orientadas de forma aleatória

COMPARAÇÃO COM DADOS EXPERIMENTAIS (tentativa)

Legenda: Exp. = experimental Num. = numérico Analít. = analítico (Dunn et al., 1993)

COMPÓSITOS COM FIBRAS DO TIPO DKA X (cond. longitudinal)									
T (K)	55%			65%			75%		
	Exp.	Num.	Analít.	Exp.	Num.	Analít.	Exp.	Num.	Analit.
293,15	50,12	64,37	69,44	66,58	29,73	101,06	71,15	53,88	152,31
313,15	49,64	58,87	63,92	66,06	26,98	93,32	71,00	49,04	141,34
333,15	49,14	60,72	65,78	65,09	27,90	95,94	70,50	50,66	145,06
353,15	48,22	62,56	67,62	64,70	28,82	98,52	70,00	52,28	148,72
373,15	46,49	67,97	73,00	62,13	31,55	106,04	69,60	57,08	159,30

COMPARAÇÃO COM DADOS EXPERIMENTAIS (tentativa)

Legenda: Exp. = experimental Num. = numérico Analít. = analítico (Dunn et al., 1993)

COMPÓSITOS COM FIBRAS DO TIPO DKA X (cond. transversal)									
T (K)	55%			65%			75%		
	Exp.	Num.	Analít.	Exp.	Num.	Analít.	Exp.	Num.	Analít.
293,15	6,80	3,41	3,21	9,10	5,51	4,39	7,83	14,46	6,50
313,15	6,80	3,08	2,90	9,08	4,98	3,96	7,81	13,09	5,88
333,15	6,76	3,19	3,00	8,97	5,15	4,10	7,79	13,55	6,08
353,15	6,75	3,30	3,10	8,80	5,33	4,25	7,79	14,00	6,29
373,15	6,65	3,63	3,41	8,80	5,86	4,67	7,74	15,37	6,92

ARRANJO DESORDENADO DE CILINDROS COM RESISTÊNCIA TÉRMICA INTERFACIAL E POROS (c_p = 0,5%) (novidade!)

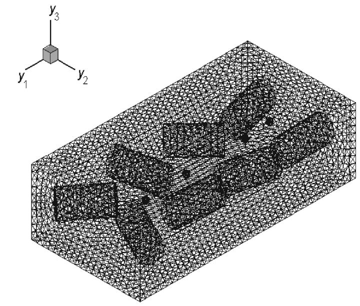

Caso teste 1: α = 250 e Bi = 10

Caso teste 2: α = 250 e Bi = 10^{-6}

Caso teste 3: $\kappa_{11} = \kappa_{22} = \kappa_{33} = 250$, $\kappa_{12} = \kappa_{13} = \kappa_{23} = 200$ e Bi = 10

Caso teste 4: $\kappa_{11} = \kappa_{22} = \kappa_{33} = 250$, $\kappa_{12} = \kappa_{13} = \kappa_{23} = 200$ e Bi = 10^{-6}

Caso teste	Condutividade térmica efetiva c = 13% e ρ_f = 1,5		
	$\kappa_{11}^{e,h}$	$\kappa_{22}^{e,h}$	$\kappa_{33}^{e,h}$
1	1,299	1,189	1,083
2	0,8649	0,8497	0,8336
3	1,282	1,180	1,080
4	0,8650	0,8497	0,8336

POSSÍVEIS TRABALHOS FUTUROS

- Implementação de modelos geométricos em 3-D mais representativos de microestruturas de materiais compósitos

- Implementação de uma resistência térmica interfacial variável ao longo da superfície das fibras (Duschlbauer et al., 2003; Fletcher, 2001)

- Tratamento apropriado da microescala para análise de microestruturas nas configurações bem próximas à máxima concentração e com resistência interfacial finita entre as fases

- Extensão da metodologia desenvolvida à determinação de propriedades mecânicas efetivas de materiais compósitos (por exemplo, módulo de elasticidade efetivo)

- Consideração do efeito da variação das propriedades com a temperatura

JOURNAL OF THERMOPHYSICS AND HEAT TRANSFER
Vol. 15, No. 1, January-March 2001

Homogenization of Temperature-Dependent Thermal Conductivity in Composite Materials

Peter W. Chung* and Kumar K. Tamma†
University of Minnesota, Minneapolis, Minnesota 55455
and
Raju R. Namburu‡
U.S. Army Research Laboratory, Aberdeen Proving Grounds, Maryland 21005

Of the various homogenization approaches, the asymptotic expansion homogenization (AEH) approach for homogenizing nonlinear composite material properties continues to grow in prominence due to its ability to handle complex microstructural shapes while relating continuum fields of different scales. The objective is to study the AEH approach for nonlinear thermal heat conduction with temperature-dependent conductivity. First, two approaches are proposed to investigate the sensitivity of the homogenized conductivity to higher-order terms of the asymptotic series. Under conditions of symmetry such as in unidirectional composites, the two approaches give the same homogenized properties. Then validations are shown for unidirectional composites for changing volume fraction and temperature. The validations are performed using measurements and analytical formulas available in the literature. The findings show good agreement between the present numerical predictions and independent results. Finally, a simple nonlinear steady-state heat conduction problem is demonstrated to illustrate the multi-scale procedure. The numerically predicted results are verified using a Runge-Kutta solution.

Although limited developments are available in homogenization of linear conductivity,[9,10] no efforts to date have treated the nonlinear temperature dependence of conductivity or shown how such approaches substantiate the results.

The smaller the magnitude of ε, the smaller the influence of the macrolevel temperature gradients on the microscale homogenized properties. Under certain conditions, the difference between the approaches is nominal. Conditions when the linearized and nonlinear homogenization equations yield identical or nearly identical results are 1) the microstructural geometry contains symmetries, 2) the material is homogeneous, 3) $\partial T^{(0)}/\partial x = 0$, and 4) $\varepsilon \lll 1$.

In summary, the steps in the proposed linear and nonlinear computational procedures are enumerated as follows.

Linear

The linear approach assumes that the temperatures are constant in Y. The procedure for determining the homogenized conductivity in a finite element sense is as follows:

1) Compute the macrotemperature distribution.

2) Determine the element average (at centroid or integration points) temperatures for each macrolevel element.

3) Determine the individual phase conductivities at the average temperature at each microlevel element.

4) Solve the auxiliary equation (10) for χ^j using the conductivities from step 3.

5) Use the solution for χ^j in Eq. (15) to determine the effective conductivity of the macroelement.

Nonlinear

The nonlinear approach makes no restrictions on the temperature distribution in Y. This results in a nonlinear dependence of the homogenized conductivity on the local temperature fields. The procedure to determine the effective conductivity is as follows:

1) Compute the macrotemperature distribution.

2) Determine the element average (or centroid or integration points) temperatures for each macrolevel element.

3) Solve for χ^j in Eq. (12) using the conductivity values for the present iteration.

4) Determine the microscale temperatures using the first two terms in Eq. (4).

5) Update the conductivities of the constituents using the microscale temperatures.

6) Loop back to step 1 until χ^j converges.

7) The effective conductivity is then computed from the converged corrector functions χ^j.

ALGUNS TRABALHOS PUBLICADOS ATÉ O MOMENTO

- Matt, C. F. and Cruz, M. E., 2004, Calculation of the effective conductivity of disordered particulate composites with interfacial resistance, Proc. 37th AIAA Thermophysics Conference, Portland, Oregon, AIAA 2004-2458, pp. 1 – 12

- Matt, C. F. and Cruz, M. E., 2004, Enhancement of the thermal conductivity of composites reinforced with anisotropic short fibers, submitted to Journal of Enhanced Heat Transfer

- Matt, C. F., 2003, Condutividade térmica efetiva de materiais compósitos com microestruturas tridimensionais e resistência térmica interfacial, Tese de Doutorado, COPPE/UFRJ, Programa de Engenharia Mecânica

- Matt, C. F. and Cruz, M. E., 2002, Application of a multiscale finite-element approach to calculate the effective conductivity of particulate media, Computational and Applied Mathematics, vol. 21, pp. 429 – 460

- Matt, C. F. and Cruz, M. E., 2002, Effective conductivity of longitudinally-aligned composites with cylindrically orthotropic short fibers, Proc. 12th International Heat Transfer Conference, Grenoble, France, vol. 3, pp. 21 – 26

- Matt, C. F. and Cruz, M. E., 2001, Calculation of the effective conductivity of ordered short-fiber composites, Proc. 35th AIAA Thermophysics Conference, Anaheim, California, AIAA 2001-2968, pp. 1 - 11

Cálculo das contribuições associadas ao nó mediano *M* em Γ

- Definição da função peso $v_M|_{e,\Gamma} = \phi_M^c|_{e,\Gamma}$
- Cálculo do salto da função peso $[v_M]_{\Gamma_{ee'}} = v_M|_{e,\Gamma} - \overbrace{v_M|_{e',\Gamma}}^{0} = \phi_M^c|_{e,\Gamma}$
- Cálculo do salto da função teste $\left[\chi_{p,h}^{\mathrm{II}}\right]_{\Gamma_{ee'}} = \chi_{p,h}^{\mathrm{II},c}|_{e,\Gamma} - \chi_{p,h}^{\mathrm{II},d}|_{e',\Gamma}$

$$\left[\chi_{p,h}^{\mathrm{II}}\right]_{\Gamma_{ee'}} = \chi_A\,\phi_A^c|_{e,\Gamma} + \chi_B\,\phi_B^c|_{e,\Gamma} + \chi_C\,\phi_C^c|_{e,\Gamma} + \chi_M\,\phi_M^c|_{e,\Gamma} + \chi_N\,\phi_N^c|_{e,\Gamma} + \chi_P\,\phi_P^c|_{e,\Gamma} -$$
$$\chi_{A'}\,\phi_{A'}^d|_{e',\Gamma} - \chi_{B'}\,\phi_{B'}^d|_{e',\Gamma} - \chi_{C'}\,\phi_{C'}^d|_{e',\Gamma} - \chi_{M'}\,\phi_{M'}^d|_{e',\Gamma} - \chi_{N'}\,\phi_{N'}^d|_{e',\Gamma} - \chi_{P'}\,\phi_{P'}^d|_{e',\Gamma}$$

somar ao componente K_{MA}

$$\int_{\Gamma_{ee'}} \mathrm{Bi}\,[v_M]_{\Gamma_{ee'}}\,\left[\chi_{p,h}^{\mathrm{II}}\right]_{\Gamma_{ee'}} d\mathbf{s} = \mathrm{Bi}\Bigg(\chi_A \boxed{\int_{\Gamma_{ee'}} \phi_M^c|_{e,\Gamma}\,\phi_A^c|_{e,\Gamma}\,d\mathbf{s}} + \chi_B \int_{\Gamma_{ee'}} \phi_M^c|_{e,\Gamma}\,\phi_B^c|_{e,\Gamma}\,d\mathbf{s} +$$
$$\chi_C \int_{\Gamma_{ee'}} \phi_M^c|_{e,\Gamma}\,\phi_C^c|_{e,\Gamma}\,d\mathbf{s} + \chi_M \int_{\Gamma_{ee'}} \phi_M^c|_{e,\Gamma}\,\phi_M^c|_{e,\Gamma}\,d\mathbf{s} + \chi_N \int_{\Gamma_{ee'}} \phi_M^c|_{e,\Gamma}\,\phi_N^c|_{e,\Gamma}\,d\mathbf{s} +$$
$$\chi_P \int_{\Gamma_{ee'}} \phi_M^c|_{e,\Gamma}\,\phi_P^c|_{e,\Gamma}\,d\mathbf{s} - \chi_{A'} \int_{\Gamma_{ee'}} \phi_M^c|_{e,\Gamma}\,\phi_{A'}^d|_{e',\Gamma}\,d\mathbf{s} - \chi_{B'} \int_{\Gamma_{ee'}} \phi_M^c|_{e,\Gamma}\,\phi_{B'}^d|_{e',\Gamma}\,d\mathbf{s} -$$
$$\chi_{C'} \int_{\Gamma_{ee'}} \phi_M^c|_{e,\Gamma}\,\phi_{C'}^d|_{e',\Gamma}\,d\mathbf{s} - \chi_{M'} \int_{\Gamma_{ee'}} \phi_M^c|_{e,\Gamma}\,\phi_{M'}^d|_{e',\Gamma}\,d\mathbf{s} - \chi_{N'} \int_{\Gamma_{ee'}} \phi_M^c|_{e,\Gamma}\,\phi_{N'}^d|_{e',\Gamma}\,d\mathbf{s} -$$
$$\chi_{P'} \int_{\Gamma_{ee'}} \phi_M^c|_{e,\Gamma}\,\phi_{P'}^d|_{e',\Gamma}\,d\mathbf{s}\Bigg)$$

CÁLCULO DAS INTEGRAIS DE SUPERFÍCIE RESULTANTES

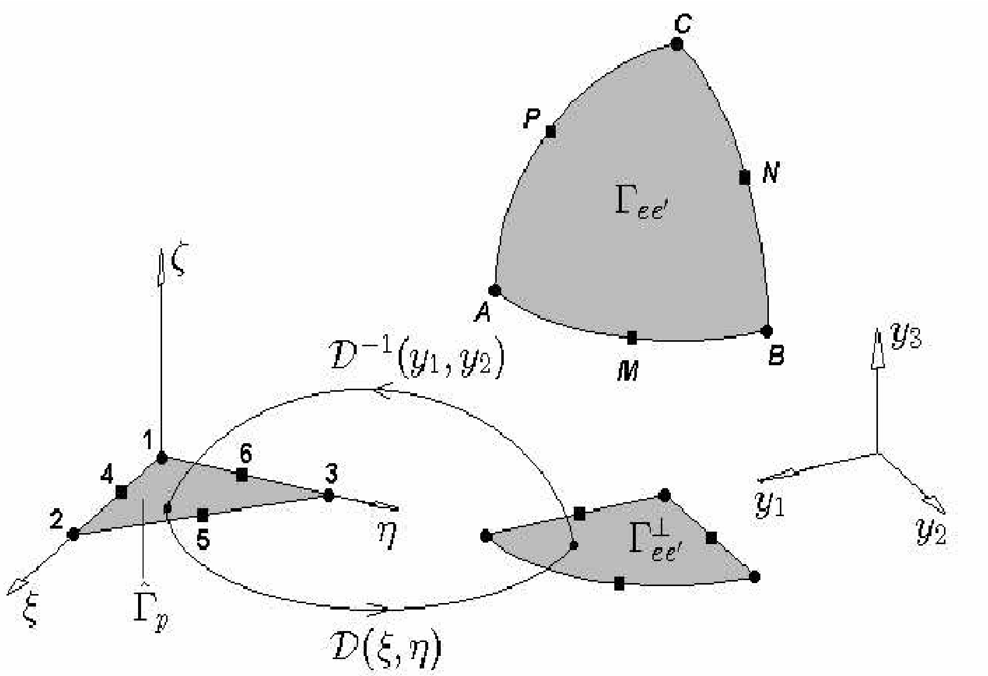

$$\Delta(\xi,\eta) \equiv (\partial f/\partial y_1)$$

$$\Omega(\xi,\eta) \equiv (\partial f/\partial y_2)$$

$$\int_{\hat{\Gamma}_p} \varrho(\xi,\eta)\, d\xi\, d\eta \equiv \int_0^1 \int_0^{1-\xi} \varrho(\xi,\eta)\, d\eta\, d\xi$$

$$\int_{\Gamma_{ee'}} \phi^c_A|_{e,\Gamma}\, \phi^c_A|_{e,\Gamma}\, ds \quad \Rightarrow \quad \int_{\Gamma^{\perp}_{ee'}} \phi^c_A|_{e,\Gamma^\perp}(y_1,y_2)\, \phi^c_A|_{e,\Gamma^\perp}(y_1,y_2) \sqrt{1+\left(\frac{\partial f}{\partial y_1}\right)^2+\left(\frac{\partial f}{\partial y_2}\right)^2}\, dy_1\, dy_2 \quad \Rightarrow$$

$$\int_{\hat{\Gamma}_p} \phi^c_A|_{e,\Gamma^\perp}(y_1(\xi,\eta), y_2(\xi,\eta))\, \phi^c_A|_{e,\Gamma^\perp}(y_1(\xi,\eta), y_2(\xi,\eta)) \sqrt{1+\Delta(\xi,\eta)^2+\Omega(\xi,\eta)^2}\, \det \mathbf{J}\, d\xi\, d\eta =$$

$$\int_{\hat{\Gamma}_p} h_1(\xi,\eta)\, h_1(\xi,\eta) \sqrt{1+\Delta(\xi,\eta)^2+\Omega(\xi,\eta)^2}\, \det \mathbf{J}\, d\xi\, d\eta$$

- ARRANJO CÚBICO SIMPLES DE ESFERAS COM RESISTÊNCIA TÉRMICA INTERFACIAL UNIFORME
  - Comparação com CHENG & TORQUATO (1997)
  - Gráficos de convergência do erro absoluto

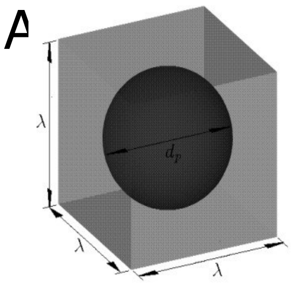

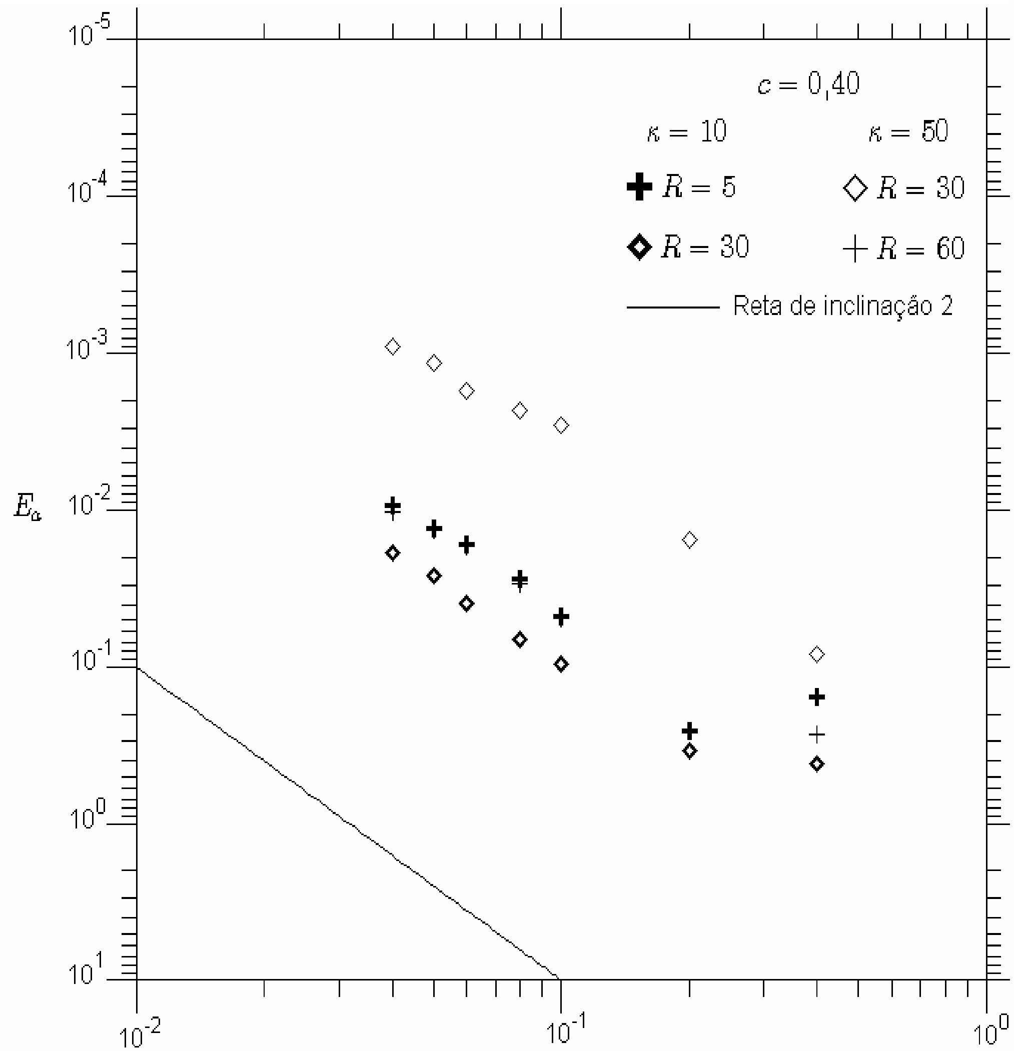

$\frac{h_0^*}{n_r}$

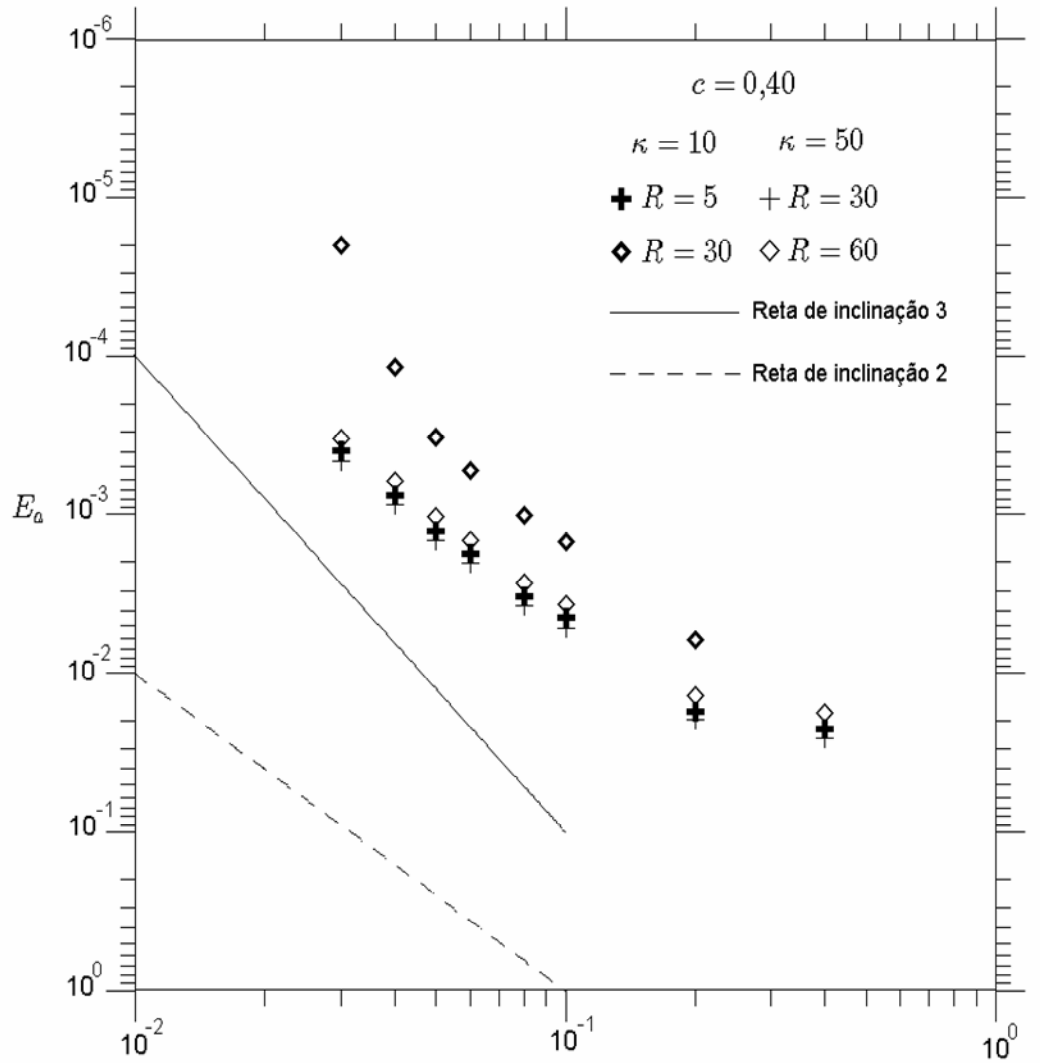

$\frac{h_0^*}{n_r}$

$$\mathrm{Bi} = 2\left(\frac{\kappa}{R}\right)\left(\frac{\pi}{6\,c}\right)^{1/3}$$